Appearances of the Haybusa2 and OSIRIS-REx target asteroids Ryugu and Bennu

A. Soumbatov-Gur

Properties and features of asteroid (101955) Bennu to be reached this fall by NASA's OSIRIS-REx probe are anticipated. As of September 2018 we reconcile distant groundwork data on the asteroid in a unified approach based on the paradigm of ejective formation of celestial bodies. Recent JAXA's observations of diamond-shaped asteroid (162173) Ryugu are also systematically considered to give grounds to Bennu's study as explosively casted out rock body. We as well analyze data on top-like main belt and near-Earth asteroids: (2867) Steins, (341843) 2008 EV5, (65803) Didymos, and others. Dozens Bennu's constraints and properties predicted include diamond shapes, North-South dichotomy, strong equatorial mountain range, curved northern relief features, global fault, regular equatorial depressions, ten meters wide crater in high southern latitudes, angular crater shapes, side difference in crater statistics, larger than expected density, recent geologic activity, lined distributions of substances and minerals, restricted positions of locally synthesized organic materials, x-ray and electromagnetic transients, etc.

Contents

1 Introduction

Origins, Spectral Interpretation, Resource Identification, and Security-Regolith Explorer (OSIRIS-REx) asteroid sample return mission at near-Earth asteroid (101955) Bennu is now gaining its full run. The NASA's probe launched in September 2016 carries a handful of scientific instruments including telescope cameras, optical spectrometers, laser altimeters, radio experiments, and x-ray spectrometer. The spacecraft as well equipped with touch-and-go regolith sample acquisition system which is the robotic arm able to collect surface materials while hovering above asteroid surfaces [1,2].

In the nearest years the mission team has to fulfill tough schedule. It is to determine gravity, mass, and shape parameters of the asteroid, thoroughly document its surface, chose safe place to collect samples, examine it down to millimeter scales, acquire regolith samples, and return the probe at the Earth in order to land the sample capsule in Utah desert in autumn 2023.

This August the approach phase of OSIRIS-REx has begun and telescopes of the probe have started their work with the first views of the asteroid as an obscure spot. Now sixty six days before the arrival we are curious to track systematically growing images in the web (e.g. at www.asteroidmission.org).

Quite a work has been done for distant analysis of the asteroid in the course of OSIRIS-REx mission preparation. As of summer 2018 researchers knew dozens of Bennu's parameters and features [1-5]. This report is an attempt to rethink observational data on Bennu and other spinning top asteroids from a unified point of view in order to predict some of Bennu's properties. The viewpoint is based on explosive ejective approach to formation of celestial bodies put forward in [6]. There it was applied to main belt asteroid (2867) Steins with the purpose to integrally explain observations of 2008 ESA Rosetta probe fly-by.

In the following we begin with general information about our approach and its consistency with recently published results. Then we try its competence on several main belt and near-Earth asteroids. Special attention is paid to fresh data on asteroid Ryugu being now escorted by JAXA's Haybusa2 spacecraft. Further we evaluate known groundwork facts about Bennu, give some constraints on them, and predict a dozen of asteroid properties. We also discuss the implications of ejective approach and speculate on parent bodies of Ryugu, Bennu, and other near-Earth asteroids. Finally we briefly put our rationale into broad scientific and historical frames.

2 General scheme of asteroid genesis

2.1 Ejections with simultaneous crater creations

The basics of new explosive ejective approach to celestial rocky objects' genesis were proposed on example of asteroid (2867) Steins in [6]. The model naturally results from the phenomenology of ejective orogenesis as well as data on asteroids and statistical facts about their families. Ubiquitous among rigid celestial bodies phenomenon of ejective orogenesis was described on example of asteroid (1) Ceres in [7]. Brief overview of explosive ejective orogenesis on expanding and geologically active dwarf planet Ceres is also given in [6].

In its course a conical or pyramid-like mountain forms inside parent crust as a result of crack and fault development. Then the mountain is explosively casted rotated out of parent body with simultaneous crater creation and severe modifications of local materials. The ejected body usually falls not far from newly appeared crater or disrupts into several or many parts.

The ejection is usually mediated by dyke streak evolvement on crater walls. Dyke remnants on crater/mountain surfaces are prone to be spiral. Their curvatures are the results of local crustal shears leading to plasticity. The curvatures' shape manifests clockwise or anticlockwise rotational direction of ejected mountain. The only logical step from ejective orogenesis to ejective asteroid genesis is the guess of opportunity for an ejected body to overcome parent gravity.

While analyzing explosive ejective geneses two tendencies being sides of the same coin should be kept in mind. The one is strong genetic relations between parent and offspring rocks. Descendents retain lots of features and parameters of ancestors as former parts of their crusts. The opposite tendency is severe shock and high temperature modifications of both bodies along the separation surfaces and deep bulk modifications of offspring rock. This way the ejection laws predetermine the properties of rock bodies brought out and their future evolution.

Herein we present examples of ejected bodies on Ceres and craters on Mars and the Moon in order to describe essential features. Fig.1 (left) gives the image of Ceres' copious cone-like mountains in the size range of all asteroids discussed in this work, except for Lutetia. The central biggest elliptical (7x8 km) mountain is approximately of the size of asteroid Steins [6]. The mountain is divided by remains of its main fault along minor axis which ends near perimeter with singular region [7]. The innate to the orogeneses region appear to be the result of largest local modifications due encounter of circling detonation waves at formation moment. The main fault groove of the cone mountain is curved counterclockwise fig.1 (left). The perimeter and slopes look a bit wavy because of dyke remnants and include brighter fresh materials. The cone mountain elongation results from crustal plastic deformations and subsequent rebound after ejection [7].

Fig.1 (right) shows fresh 2.2km wide crater Linne located in lunar Mare Serenetatis. There are boulder rings around it and a brighter mountain of similar size north of it. Linne's bright materials and concentric rays are typical of new lunar craters of all sizes. Concentric rings of different widths and colors are marks of borders of crustal layers, the upper being the narrower. The central region of crater is also somewhat elongated vertically (relative to page borders).

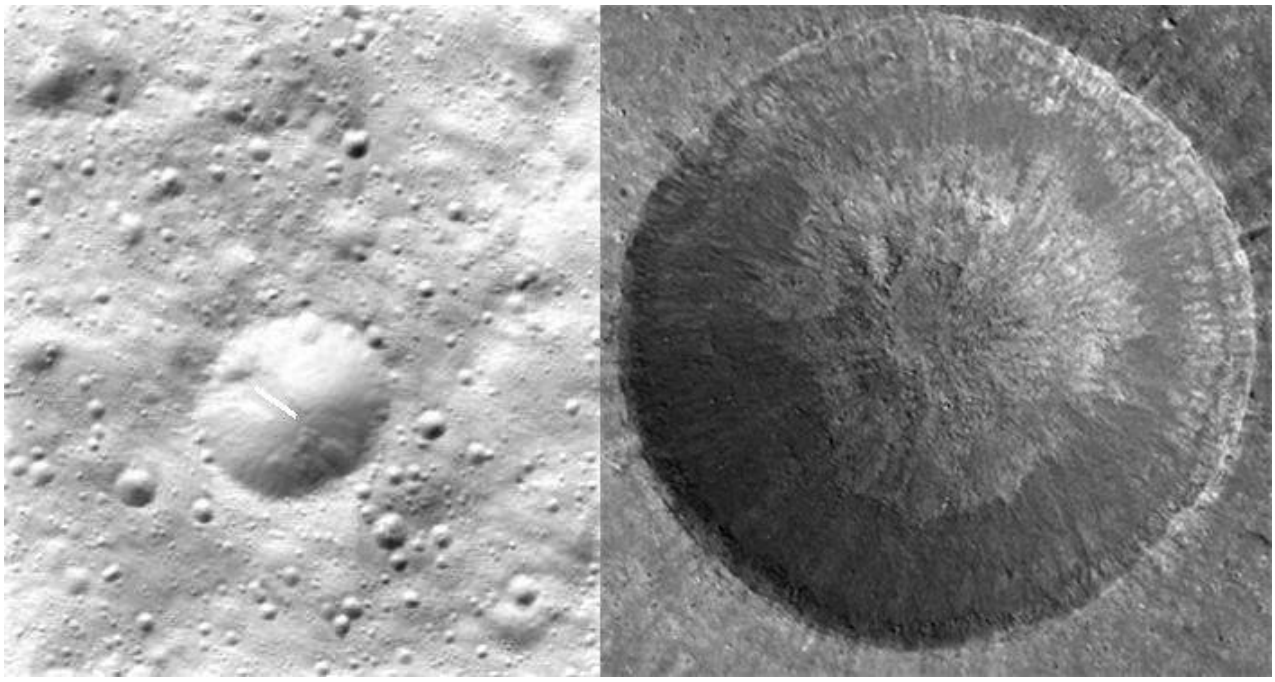

Fig.1. Left: A view.of Ahuna region located close to equator of Ceres. It is cropped from NASA's pia20348 view. The background was subtracted and contrast was enhanced by us. The largest cone mountain is approx.7x8km in size. Notice slope striations and perimeter waviness. The view was acquired by Dawn probe from the low altitude mapping orbit 385km above the surface. White line marks main fault groove. Right: Linne lunar crater 2.2km wide from NASA's LROC view NAC M122129845
(http://www.jpl.nasa.gov/spaceimages/details.php?id=PIA20348, https://commons.wikimedia.org/wiki/File:Linne-lroc.jpg)

Analyses of Lunar Reconnaissance Orbiter data [8] demonstrate that Linne is canonical crater in mare Fe-Ti-rich basalts. It is not bowl-shaped as previously thought, but best approximated by a truncated cone. The normalized crater volume to surface area divided by total crater depth (0.368) is similar to (0.372) for Danny Boy basalt event in Nevada, but lower than those digits for most craters on the Moon, Mars, and Earth. The article [8] proves that minimally-modified simple craters on the Moon and Mars display similar geometric properties, despite differences in gravity. Linne is a landform with characteristics that can be used as reference point for comparisons with other pristine landforms on the Moon, Mars, and Earth. Thus the analyses of [8] support gravity independence of our approach.

Fig 2 (left) presents the view of a pedestal crater in Amazonis region of Mars. Dark concentric rays seen in the crater are not surprising from our ejective viewpoint. The rays are the dyke streaks, seemingly with high carbon contents. Pedestal rays are less developed and covered with ejecta. Singular region also exists. Fig 2 (right) shows a weird conical cavity on southern flank of large Martian shield volcano Pavonis Mons. A hundred and half meters wide hole was discovered by the HiRISE instrument aboard the NASA's robotic Mars Reconnaissance Orbiter. The hole is thought to be an opening to a cavern that was covered on top by solidified lava flows. It was proposed that cone material disappeared via bottom pit into deep underground cave. Why there is circular crater surrounding this hole remains a topic of speculations.

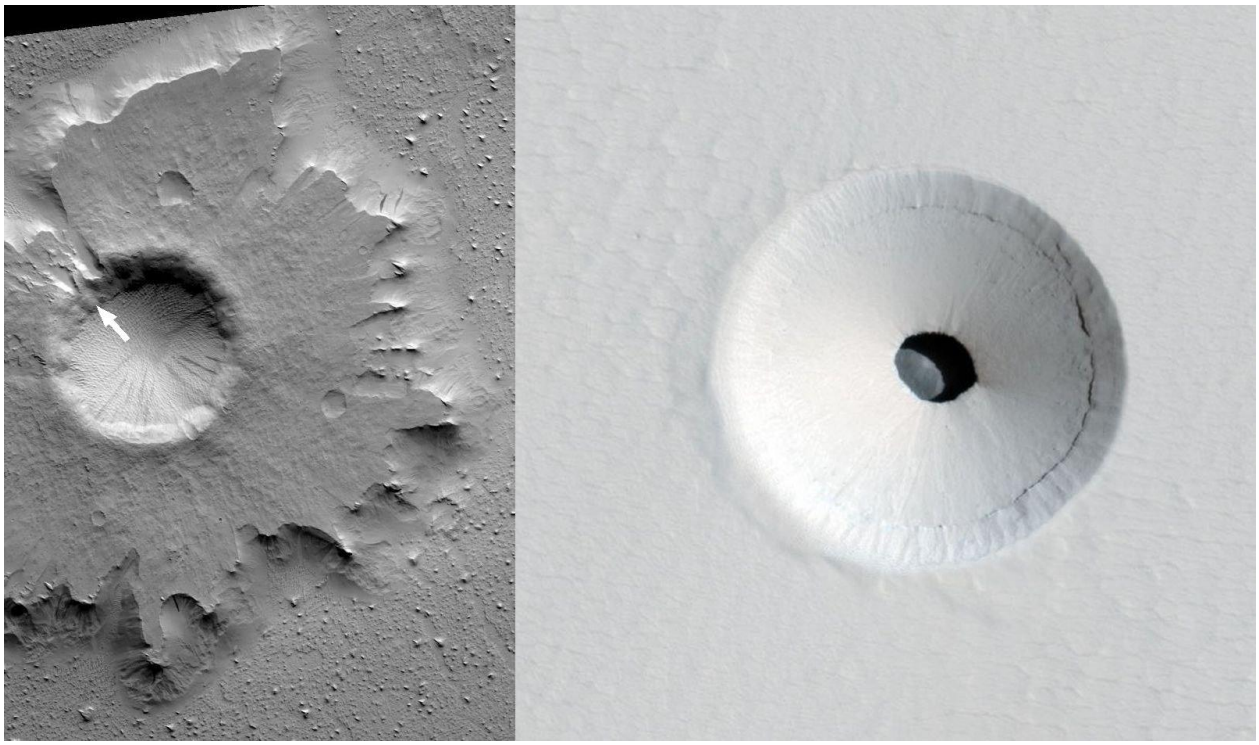

Fig.2. Left: Image of crater with dark concentric streaks on plain pedestal in Amazonis region of Mars (7.3 north latitude, 164.4 west longitude). White arrow marks the region of singularity. Right: Image of hundred meters wide conical hole on the slope of Martian Pavonis mons shield volcano. It is a crop from Astronomy picture of the day (2012 July 18). Notice black material ring concentric with the perimeter which reveals the crossing of slope with surface layer border. Bright crescent in central dark pit marks solar shadow in the partly illuminated area. (https://commons.wikimedia.org/wiki/File:Pedestal_crater_and_streaks.jpg, https://apod.nasa.gov/apod/ap120718.html)

Our approach to crater/caldera formation is the same for plane and corrugated relief areas e.g. volcanic edifices incl. their summits or slopes. We are sure the conical crater originated due to crack development. The elliptical hole and a dark ray along its major axis prove that. Almost ideal cone with ca. circular base appears to result from local fracture of very strong lava layers solidified on dusty slopes of Pavonis Mons. The black bottom hole, rings, and rays are supposed to be explosively modified substances with high carbon contents.

Indirect and statistical proves of explosive ejections are numerous [6,7] and we are discussing some of them in the next Section. The direct proves of both ejective orogenesis and ejective asteroid genesis should be infrequent in recent tranquil stage of Solar System evolution. Suffice it to say that contemporary rate of small crater formation on Mars is about twenty per year. For larger ejected bodies large explosive transients are to be rarer.

But in our times when the sky is spacecraft patrolled and telescope controlled in the widest range of wavelengths direct proves are also abundant. The problem is to distinguish them among a whale of facts unnoticed, rejected, or interpreted different way. We think the analyses of bursts in different spectral ranges as well as numerous transient phenomena on the Moon and Earth may be of great help.

2.2 On the mechanism of ejections and disruptions

Today's asteroid science has a lot of fundamental shortcomings. It is said in [9] that interrelations of short-range strength and long-range gravity give intricate mechanical balance which is only partly understood: "Instead of competing for dominance, strength and gravity collaborate over a wide spectrum of sizes and shapes to produce some of the richest structures in nature."

Contemporary standards of asteroid modeling are hydrocode simulations of their disruptions and ejections due to outer random impacts. The theory contradicts to orbital asteroid evolutions because it leads to high initial ejection velocities that require strong outer impacts which are to destroy parent bodies [10]. Vice versa, diminutive outer impacts save the integrities of parent bodies but do not result in proved ejection velocities of newly formed asteroids.

Our ejective approach leads to a number of obvious qualitative conclusions which are consistent with observations. According to it destructions of solid celestial bodies are the results of nonlinear interactions of their mechanical eigenmodes. That is we consider asteroids and their parts as open systems with energy incomes and outcomes. When the energy of excited solid rock media canalizes into prevalent modes instability develops. If its space spectrum i.e. the range of excited space wave vectors is narrow only one of mode wavelengths survives and predetermines the size scale of an ejected offspring. This way its size is naturally related to that of parent body. The instability may lead to disruption into several large parts or in case of high energy income even to overall asteroid explosion. Separations always happen along stress concentrating inner asteroid borders e.g. cracks, faults, inclusions, etc. Small energy income results in slowly growing shape corrugations mediated by inclusion diffusions which we grasp as plasticity.

The mechanical modes are hierarchically connected to each other. That is reflected in overall shapes of celestial bodies as well as in their fault maps from global scales down. The connection implies identical self-sustainable instability mechanism of inclusion diffusion and substance formation reactions with simultaneous displacements and deformations for different scales of lengths. This generalization means that main features of the process of celestial bodies' formation and evolution do not depend on their sizes. Thus, the ejective approach is scale invariant i.e. it embraces celestial rock's size range of approx. a dozen orders of magnitude.

It is known that regimes of impact crater formation in hydrocode models are suspicious or even inconsistent with mechanical properties of asteroids. Collision impact evolution does not explain survival of large craters on asteroids [9]. Such craters are commonalities for asteroids. The usual theoretical conclusion is that after strong impact the target is to finally become rubble pile.

Our model elucidates the situation. Large craters which trend to be half of parent's size are the results of mechanical excitation of the first mode (second after zero fundamental overall). Its wavelength is twice less than parent body's size (see also [6]). When explosively ejected with simultaneous crater formation an offspring does not produce strong recoil reaction in a parent due to low mass ratio, masses being proportional to sizes cubed.

It is commonly thought that given weak cohesion of rubble pile asteroids the regime of gravitational and centrifugal force compensation due to Yarkovsky–O'Keefe–Radzievskii–Paddack (YORP) spin-up is able to explain disruptions of asteroids in size range 0.25-10km [11]. Our approach is an alternative explanation of that asteroid statistics in the range due to effortless disruptions and casting out parts of strong rock bodies resulted from inner fracture processes.

The problems of asteroid modeling are not strange. Asteroid low gravity made our Earth-based intuition unrelated. For instance structurally weak asteroids and comets sometimes are highly resistant to catastrophic disruption throw stress dissipation [9]. That effect is normal in the frames of our nonlinear model. The dissipation realizes through nonlinear interactions of stress modes, by other words, through plasticity mediated by strain stimulated diffusion and substance modifications.

Other drawback of asteroid science is classification unreliability which means that same spectral class does not guarantee same material contents of asteroids. Spectra may be the mixes of rocks formatted under severely different thermal conditions [9]. The conclusion is direct outcome of our approach. Explosive ejective modifications of asteroid surfaces are possible to be numerous, sometimes ruthless, and even produce igneous rocks of different kinds. Minimally an ejected body has to have striking North-South dichotomy.

Recent publication about common origin of family and non-family main belt asteroids also supports our ejective approach [12]. It was found that sizes of main belt asteroids are correlated with proper orbital eccentricities and anticorrelated with proper inclinations. Given actual asteroid size distribution these trends made the authors to conclude that main belt asteroids are the descendents of several large parent bodies.

Our ejective model offers the same evolution conclusion for sequential offspring generations and accounts for the above correlations the following way. Initial starting velocity determines flight distance or eccentricity of explosively thrown out object. Vertical and equatorial starts are the most effective for orbital and outward ejections. When a body is ejected in equatorial belt it needs less energy due to the help of centrifugal forces. Equatorial starts that even in Earth's case provide energy gains are possible to drastically down potential barriers of much smaller parent bodies. By other words, vertical ejections outside equator region took more energy for the same body size.

Generally speaking the energy of global mechanical excitation may be canalized into ejection all over the parent body. But for starts outside equator the same explosive energy sends smaller objects into space. Thus asteroids ejected into more inclined orbits tend to be less sizable. In the final run parent body acts as a rotating slingshot which sends celestial objects into their orbits around the Sun. It is clear that offspring orbits tend to concentrate in equatorial planes of their parents.

As for the eccentricity the correlation problem is more complex. Starting trajectories of ejected rocks are not fully understood yet and some observations show that they may be very specific. But there are hints to solve the problem. The more massive is a surged up offspring body, the less disturbed is its direct trajectory due to outer forces. For instance, parental Coriolis forces are able to curve the orbit of newly born body just after start. Hence larger asteroids are prone to have higher eccentricities due to straighter starts.

3 Examples of ejected diamond-shaped asteroids

Size independence of the asteroid genesis greatly alleviates the geometrical analyses of ejected bodies. Scale invariance allows for natural comparisons of seemingly dissimilar objects orders of magnitude different in sizes, even asteroids and regolith particles. Further we apply our rationale to main belt and near-Earth asteroids of similar shapes without paying attention at their dimensions and spectral classification types.

3.1 Main belt asteroid Steins

Earlier we tried our approach to asteroid genesis on diamond-like main belt asteroid (2867) Steins [6]. We analyzed the observations acquired on 5 September 2008 by ESA's Rosetta spacecraft on its way to comet 67P/Churyumov-Gerasimenko [13,14]. The asteroid is fresh object in the sense that its shape has not changed a lot since origination. It is in initial evolution stage. Let us remind our conclusions in a few words.

Steins has cone shape of almost ideal brilliant cut diamond. That is why majority of the asteroid relief features are named after jewels (fig.3). Steins' retrograde rotational axis is the cone's symmetry one. This condition is natural for explosive ejective geneses. Spectrally Steins is E-type asteroid with igneous rocks formed around 1500°C. The asteroid dimensions along the principal axes of inertia (x,y,z) are 6.83x5.70x4.42km. There is a bit of elongation in x-axis direction compared to y one. The asteroid is divided approx. by half with the global fault remnant which produced groove on (-y) side and grooved catena (craters lined from Agate to Lapis and Diamond) on the opposite (+y).

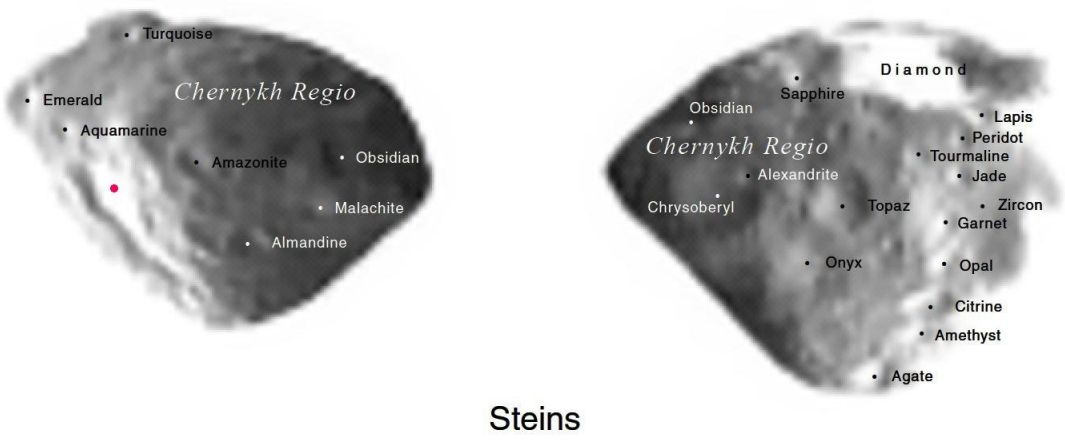

Fig.3. Map of Steins' surface features named after precious stones. The views acquired during the fly-by cover a bit more than half of the asteroid surface. The left view was taken by Rosetta before close encounter, the right one – after it. Different sizes of the views are due to the difference in distances between the asteroid and the probe. Red point marks rhombic depression (see text). (http://sci.esa.int/rosetta/54380-gemstones-on-diamond-like-steins/)

Steins is covered with tens of craters of different sizes possible to be explained by ejective orogenesis on smaller scales. The largest of them are southern pole Diamond and a wide depression on the asteroid equatorial bulge with craters Jade, Tourmaline, etc. inside. Diamond appeared due to expansion of the Steins' main fault simultaneously with large boulder ejection. Now the boulder has small Turquoise crater on its side (fig.3, left). It also originated on stress concentrating contact boundary between the boulder and the asteroid surface. The largest bulge depression is crossed by the fault remnant (see fig.3, right). It originated in singular region of the ridge along with other smaller approx. regular perimeter craters formed as a result of stress concentrations near perimeter dyke remnants.

Steins' evolution trend is the plastic elongation perpendicular to the fault plane (in x direction). There is an odd dichotomy in crater densities and cumulative distributions in (-x, -y) and (-x, y) quadrants. We explain it by tensional differences in those areas resulted from the asymmetry of plastic elongation. The extension due to still acting stress mechanisms is also proved by the lined chain of 7 or 8 craters and rhombic pit down to it (fig.3, red point). The rhomb side features appear to form due to differential rotations between the northern and southern parts of the asteroid. This is the result of excitation of the global rotational mode. By the way, the North-South dichotomy is usual for celestial bodies. Other evidences of inner stresses are angular zigzag borders of both grooves and rhomb like craters. The tendency of some Steins' relief features to be aligned in axial direction or 45° to them is consistent with bulk and surface stresses of the asteroid which are tensions and shears, their primaries being 45° to each other.

Schematic birth of Steins is shown in fig.4. Detailed northern and southern polar views of the asteroid have been lacking. They would be interesting because its northern polar view is to posses curved or even spiral relief features which usually are remnants of plastic surface modifications while rotations at the start [7]. To our opinion the preferable birth southern pole up is proved by approximately 90º northern cone summit that is connected to primary shears at 45º to tensions in a parent body's crust as well as by location of the largest Diamond crater and its counterpart boulder in southern pole region crossed by main Stein's fault. Our model states that the pole is the area of plastic crack opening.

In ideal case of ejection out of plane crustal surface with 45º primary shears geometry of a thrown out asteroid may approximately be modeled with two 90º apex cones or pyramids juxtaposed by their bases. In that case vertical asteroid section along axis of rotation is square shaped. That means the base and height dimensions are approximately equal. Plastic reshaping before the start and irregular with strain plastic rebound result in somewhat base elongation due to plastic offset [7]. The same is the reason of a tiny difference in base dimensions. Cone truncation also leads to height shortage. Thus the widths of freshly ejected asteroids are to averagely be a bit smaller than their heights (dimensions along the axes of rotation). Ejected asteroids as well has to have a bit different base dimensions (along x and y axes).

The consideration of dozen of Steins' consistent features and characteristics in [6] has confirmed the ejective rationale. Steins is by no means a rubble pile. Our scenario means that the asteroid was structured due to severe explosive modifications at the start and a bit of plastic expansion during its evolution.

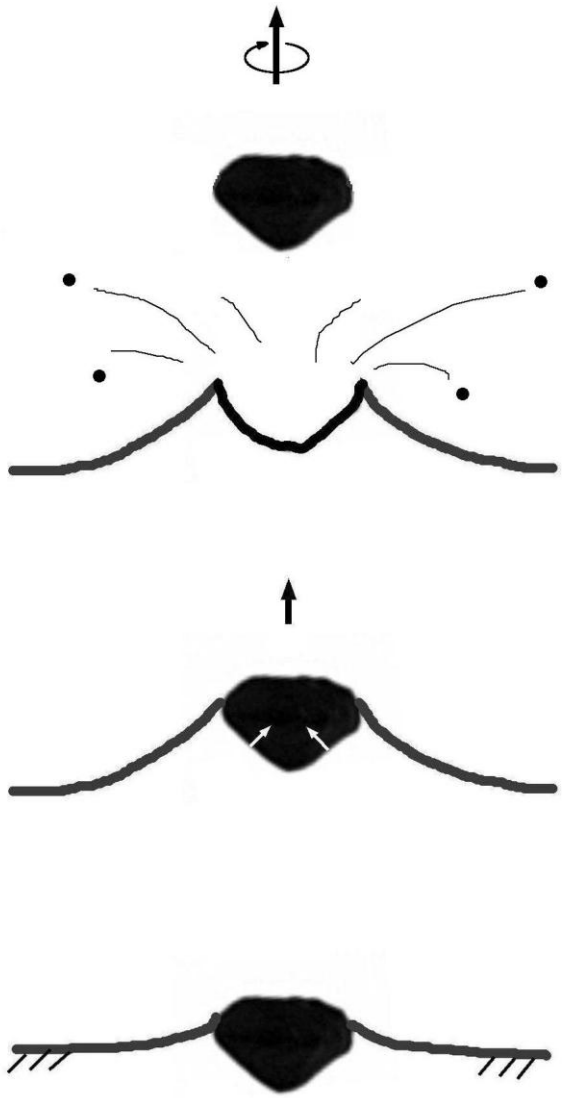

Fig.4. Steins' origination with clockwise (from above) rotation. Upper view gives the sketch of afterbirth explosive instant. Middle view shows the formation moment in mountain elevation or volcanic edifice, lower row - in plain relief region. White arrows give directions of explosive forces providing upsurge (black arrow).
(We made use of ESA's Rosetta image for figure preparation (http://www.esa.int/spaceinimages/Images/2008/09/Asteroid_Steins_A_diamond_in_space.))

There are many other main belt asteroids whose observations lead us to the conclusions analogous to the case of Steins. For instance, those are prism-shaped 5km wide asteroid (5535) Annefrank encountered by NASA's Stardust probe in 2002, or oddly shaped high density (21) Lutecia 100 km in diameter flied by ESA's Rosetta probe in 2010 (see also Discussions Section). In the following we prove that the properties of all further considered asteroids and their satellites imply the way of birth shown in fig.4. This is true undependable of sizes, masses, spectra, compositions, histories, and evolution trends.

3.2 Top-like near-Earth asteroids

Now we consider several top-like near-Earth asteroids of different dimensions and spectral classes to find their universal features before the evaluation of imaginary hazardous asteroid Bennu. Many of them were or are planned to visit by space missions. In first approximations those widespread asteroids are conical (double conical) or blob-like, sometimes a bit faceted and truncated, equatorially bulged and somewhat elongated. Radar and optical lightcurve data on them allow for distant (<0.2 A.U.) extraction of their rotational axis directions, shape details, sizes, properties of their satellites, masses, etc.

We begin with the target of rejected ESA's MarcoPolo-R sample return mission asteroid (341843) 2008 EV5. It belongs to the list of one tens of the near-Earth objects easily accessible for space missions. From a distance EV5 seems to be oblate spheroid (fig.5) [15]. Low rotation period of this 0.4km wide retrograde rotator and its lightcurve amplitude also imply that EV5's shape is not much elongated. Its most prominent feature is a ridge parallel to the equator. The equatorial ridge is broken by concavity ca. one third of the asteroid size. Other irregularities are minor. On scales smaller than tens of meters the surface is probably smooth. Large blocks are doubtful in oddities with observations of some other near-Earth objects (e.g. 2006 VV2 or 1998 CS1). On much smaller scales of centimeters to decimeters (radar wavelengths) the surface is rough. The asteroid surely has no satellites larger than 30m.

Three different methods give its maximum crustal bulk density 3.0 g/cc with 30% uncertainty. The density, combined with the optical albedo (0.12) and radar observations, is consistent with a range of normal-porosity silicate–carbonaceous and silicate–metal mixtures, i.e. with the rocky or stony-iron composition. Whether EV5 belongs to C or X asteroid class is not clear yet.

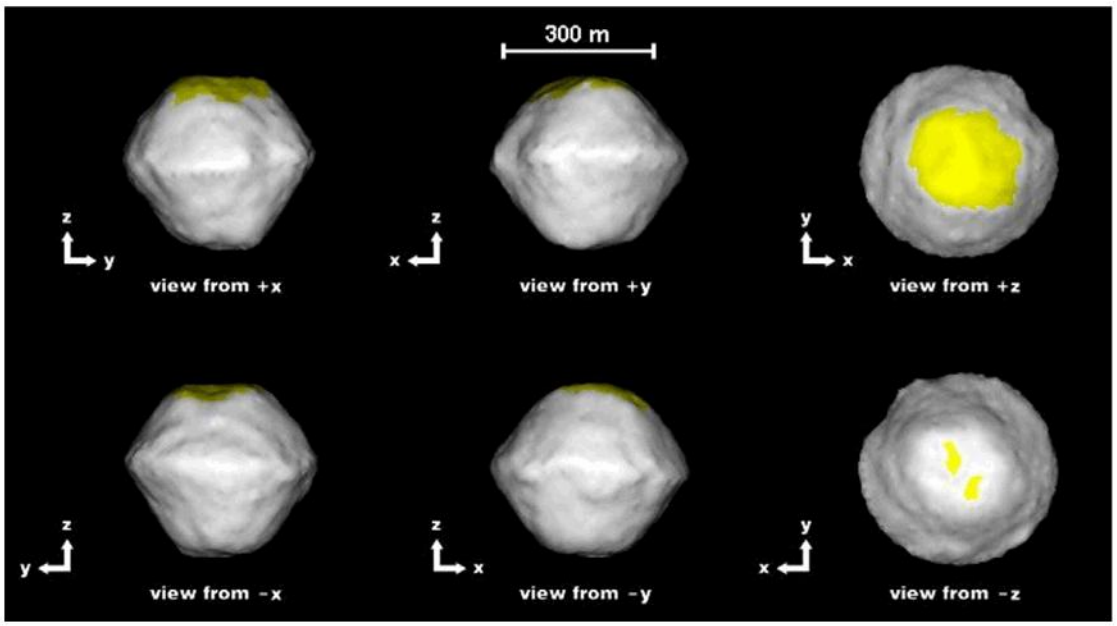

Fig.5. Modeled views of asteroid EV5 along principal axes. Z is rotation axis, its direction is that of the angular momentum vector. Yellow areas were seen only at incidence angles >45° or not seen at all.
(https://commons.wikimedia.org/wiki/File:Asteroid-2008EV5-ShapeModel-0111006.gif)

The alternative view of EV5 (fig.6) is hidden in the Supplement to [15]. Surprisingly that image with large ridge closely resembles the views of Steins. Even details of the bulge look similar to the main belt asteroid. A groove which highlights the global fault, the cause of the asteroid formation, still exists. We marked it with two black lines in fig.6. Pay attention to rhomb-like relief feature with the sides branching from the lower end of the lower black line.

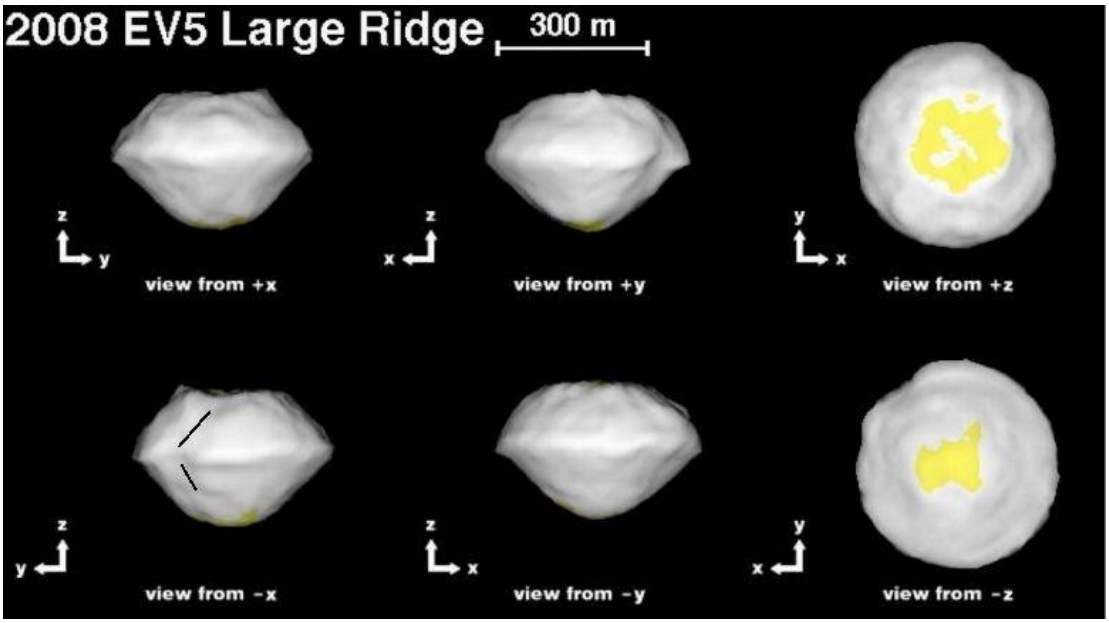

Fig.6. Alternate shape model of EV5 with large ridge. Lines mark global fault. (Fig.1 in the Supplement to [15])

The reason behind differences between the model views is that shape simulations are partly subjective. Authors of [15] "adjusted the penalty functions and selected the nominal shape to minimize the overall oblateness (the magnitude of the ridge) while also minimizing the facet-scale structure." Opposite, in fig.6 "low oblateness penalty and high penalty for facet-scale features, extends the ridge and depresses the northern pole." We prefer model of fig.6 due to inequality of the asteroid base and height dimensions.

The analysis of 2008 EV5 [15] allowed conclude that YORP effect resulted in materials' movement to equatorial areas and this way sculpted the asteroid. If the asteroid is a rubble pile, its ridge may be long ago formed by rapid rotation led to centrifugal drag. Now EV5 would have to rotate with a 2 hour period in order to reach equatorial escape velocity, as 1999 KW4 primary (see later). Recent spin is slow (period equals 3.725h) to modify the shape to the bulged one. Thus the hypothesis appeared [15] that the asteroid had drastically slowed down. The equatorial concavity is interpreted as an impact crater or, alternatively, as the result of blocks' casting out.

In the scope of our approach the asteroid looks like two cones (maybe truncated) juxtaposed by their bases. The northern view looks almost circular, while the southern polar one is elongated in the direction of (xy)-plane diagonal. It is typical (cf. figs.1,2) and reflects the asymmetry of fault development. The southern apex appears to be separated into two parts. To our opinion 2008 EV5 originated the same way as Steins. It was explosively ejected rotated and may bear shock and high temperature materials on its surface and inside.

The asteroid is not a rubble pile, the same holds for others considered in this paper. We interpret EV5 surface smoothness as the attribute of youth i.e. initial evolutionary stages which is consistent with its circular shape in (xy)-plane (cf. KW4 satellite in fig.7). Sequential evolutionary ejection/expansion modifications did not change its appearance yet. EV5 is younger than other asteroids of comparable sizes studied in this paper. Contemporary stage of Solar system evolution is calm and ejective orogenesis is active on small scales. That could be the reason of EV5 decimeter-centimeter roughness.

The equatorial structure of 2008 EV5 located at the object's potential-energy minimum is alike that of 1.5km wide primary asteroid (Alpha) of (66391) 1999 KW4 binary system. The quick spinning top-like Alpha (fig.7) is close to rotational stability limit which implies its past rotational fission. Wikipedia states that near the equator a body upped 1m above the surface would become a satellite and "the gravitational effects between the moon and the asteroid create a gigantic mountain extending in the equatorial plane around the entire asteroid". KW4 is commonly supposed to be a rubble-pile with a concavity on its bulge and with elongated satellite [16,17].

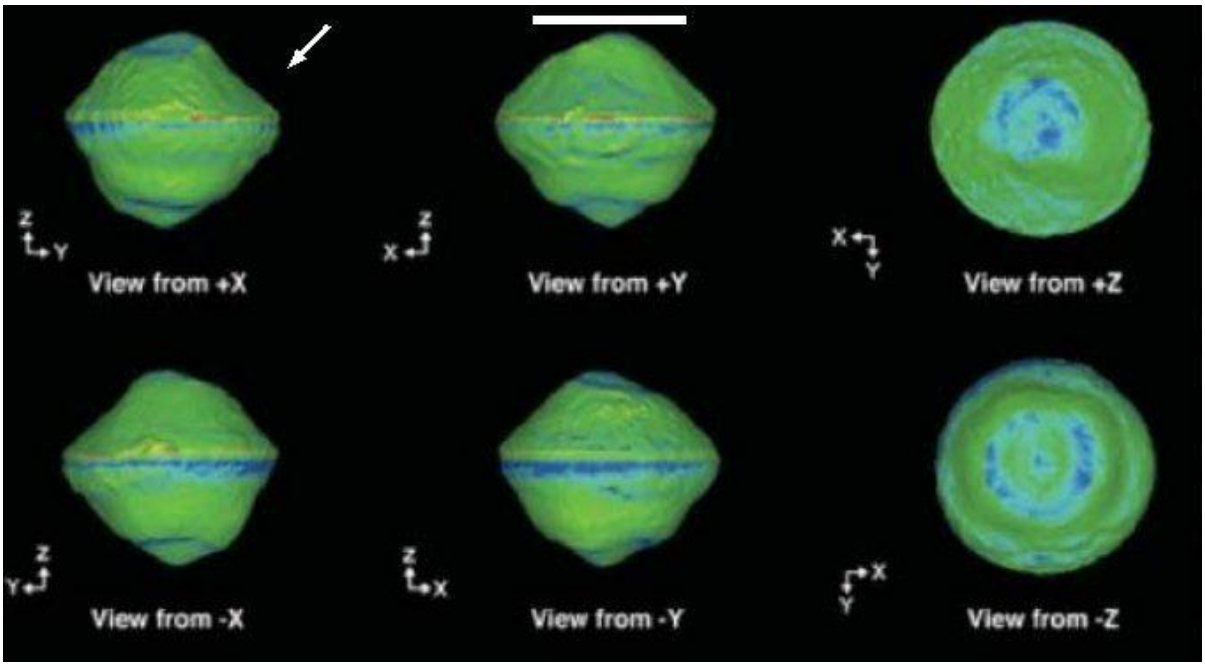

Fig.7. Axial views of KW4 primary asteroid [16]. Scale mark is 1km. Arrow points to a concavity located face-on in view from +Y. Colors from blue to red indicate calculated effective gravitational slope (0-75°).

Alpha's period is 2.8 h, density is about 2 g/cc, and porosity approx equals 50%. It is compatible with S asteroid class. The secondary (Beta) is 500m along major axis (fig.8) and bizarrely is tens percents denser. Beta's 5km in diameter circular orbit is synchronous (17.4h), the long axis of the secondary being directed to the primary. The satellite's northern pole area appears to encompass boulder-like elevation (fig.8, +Y view).

Overall shape of the satellite looks rounder and less faceted compared to Alpha due to plastic evolution, but the views along x-axis still retain cone impression (fig.7) and, at the same time, prove its expansion. The reason is that the evolution of the smaller celestial object is more rapid than the larger one.

Colors of fig.8 reflect gravitational slopes i.e. angular deviation from the local downward normal of the total acceleration vector due to gravity and rotation. Alpha's slopes average is 28° (max. 70°), whereas Beta's - 9° (max. 18°). Several times smaller average and maximal slopes prove strong evolution of the satellite and its plastic reshaping.

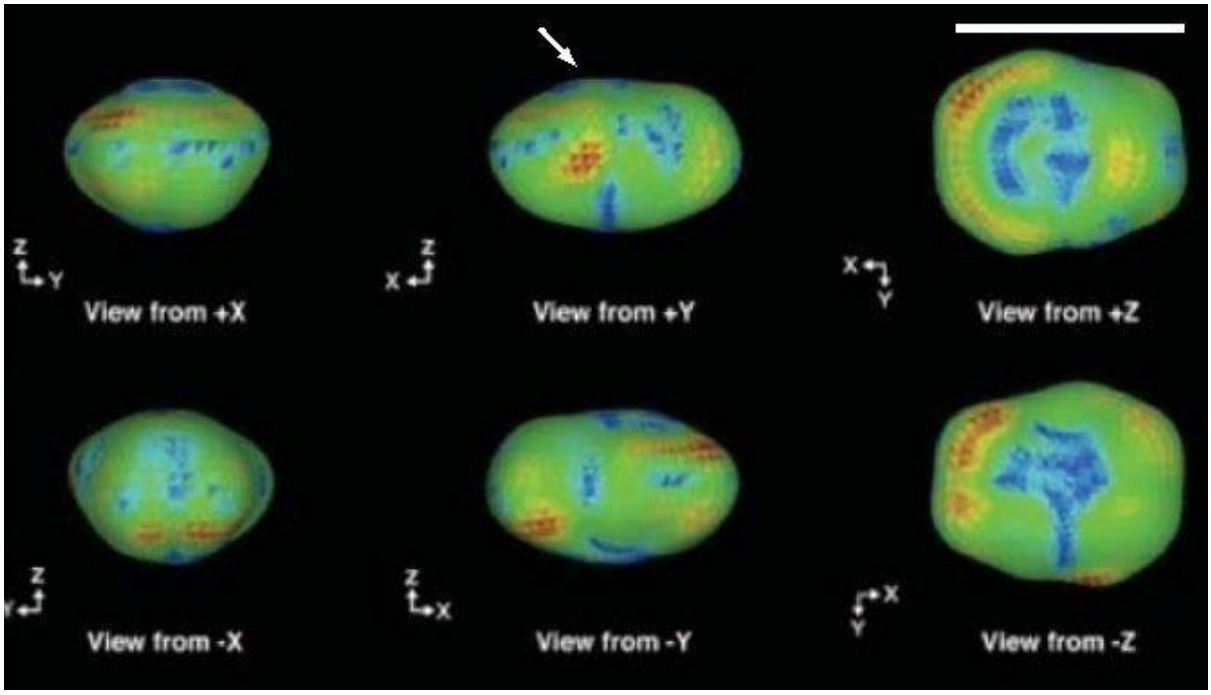

Fig.8. Axial views of KW4 satellite asteroid [16]. Scale mark is 500km. Arrow marks possible northern boulder. X axis points toward primary asteroid. Colors from blue to red indicate calculated local effective gravitational slope (0-20º). Notice that color lines are direct and often parallel to the axes.

Our explanations are the same as for EV5 or Steins. The concavity of the approximately satellite's size is the crater formed simultaneously with the ejected Beta. The density difference is explained by its formation out of dyke remnant which is not unusual to be denser. The asymmetrical elongation means that the satellite is fault divided by its minor axis and poses groove-like fault remnants on its surface. The boulder may result from polar crater formation initiated by the fault in some evolutionary stage. The orientation of color lines in fig.8 reflects overall stress symmetries.

Another interesting synchronous binary near-Earth asteroid is (65803) Didymos which revolves the sun for approx. two years and crosses the orbits of Earth and Mars. Its shape is like those of spinning tops EV5 and KV4 with equatorial sizes bigger than polar. It is a rapid rotator (2.26 h) with semimajor axis, eccentricity, and inclination equal to 1.64 A.U., 0.384, and 3.4º [18]. The supercritical rotation of the primary may imply the cohesive strength of several tens of Pascals and lose surface regolith flying off and landing down.

The average size of the asteroid is about 0.8 km. Its moon (unofficially Didymoon) is roughly five times smaller and orbits its parent for approx. 12 h. The density of the primary is 2.1 g/cc with 30% uncertainty level. 35-40% porous Didymos spectrally belongs to ordinary chondrites. According to SMASS classification it is Xk-type asteroid which transitions from the X-type to the rare K-type asteroids.

Didymos is the most easily spacecraft reachable asteroid among near-Earths. It requires less starting energy to rendezvous than that to encounter the Moon. That is why the binary system became the target of NASA's Asteroid Impact and Deflection Assessment mission which was intended to be the combination of a probe and an impact experiment planned to execute in October 2022. Didymos' small offspring is going to be aggressively hit to study the means to prevent imaginary asteroid aggression against Earth in future.

Diamond shapes are typical for primaries of near-Earth binaries. Another peculiar representative of those canonical objects with equatorial ridge, uniformly sloped sides, polar flattening, and elongated satellites is triple asteroid (136617) 1994 CC [19]. The primary asteroid looks (fig.9) like a sibling of 2008 EV5 (fig.5) but tens percents larger. Due to high eccentricity the asteroid crosses both Earth's and Mars' orbits. Optical and radar measurements provide dimensions of the primary 0.69x0.67x0.64km with 10% uncertainty, rotation period 2.38 h, Sq spectroscopic class, and light-curves of slightly elongated body with bulk density 2.1±0.6 g/cc.

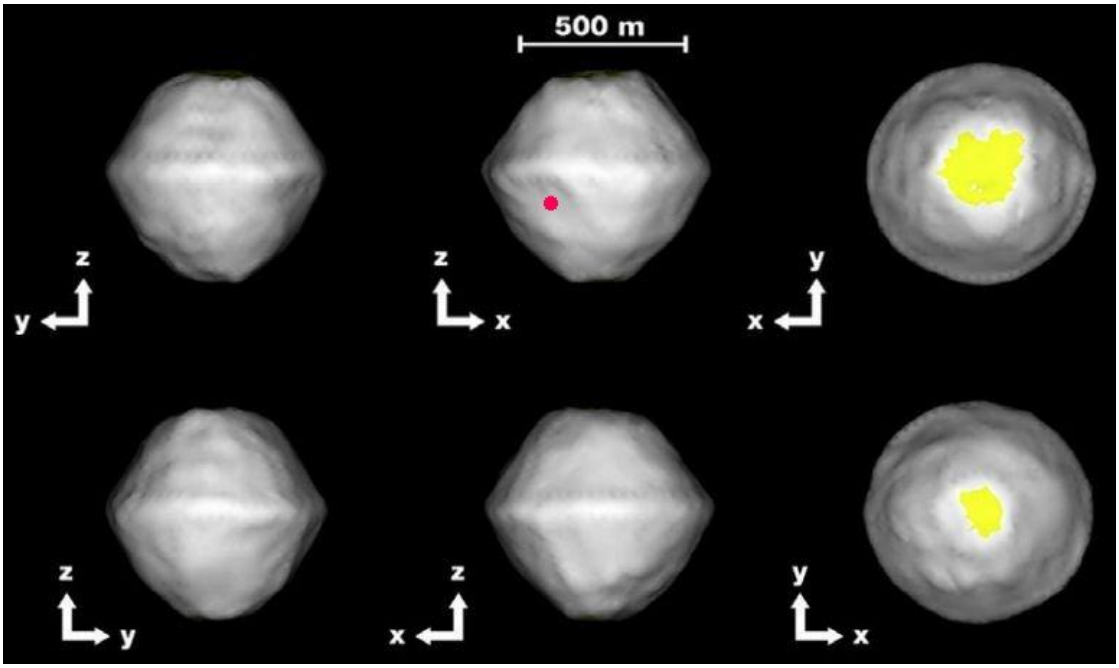

Fig.9. Axial views of 1994 CC primary asteroid [19]. Yellow color indicates areas that are not well constrained because of high radar incidence angle. Red dot marks rhombic depression resulted from differential North-South rotation.

Inner (Beta) and outer (Gamma) satellites are 112m and 80m wide with ca. 30% uncertainty. Beta has a semi-major axis of 1.7km and orbital period of 30h with slow rotation (26 ± 12h), consistent with spin–orbit lock. Beta's eccentricity is almost negligible (0.002). Gamma's semi-major axis is 5.7km which is very large for several tens known multiple. Its orbital period (9d) and rotation period (14±7h) proves the rotation is not spin–orbit locked. Gamma is six times smaller than Beta in mass, has eccentric orbit (e=0.192) inclined at16° to Beta's orbital plane.

The case of 1994 CC is common among multiple systems in the near-Earth asteroid population. Triples comprise one percent of the entire near-Earth population observed by radars. The other two clearly identified triple systems are (153591) 2001 SN263 and 3122 Florence.

4 Hayabusa2 mission at Ryugu

4.1 Groundwork data

Japan Aerospace Exploration Agency (JAXA) launched Hayabusa2 asteroid sample return mission on 3 December 2014. The target is (162173) Ryugu former 1999 JU3 [20-22]. There is close cooperation and some schedule similarity between the Hayabusa2 and OSIRIS-REx missions. Space phases of both missions are intended to continue ten years (fig.10). Six years from now material scientists will be able to compare properties of near-Earth asteroid samples in Earth's labs.

Hayabusa2 is equipped with the following scientific instruments: one telescopic and two wide-angle optical multiband cameras, near-infrared spectrometer, thermal infrared imager, laser altimeter. There is impact system to accelerate 2kg copper projectile (with high explosives inside) up to 2km/s in order to form meters-sized crater. This experiment is planned in the final mission stage after sampling touch downs. The probe also carries three small jumping rovers MINERVA-II with solar cells and a Mobile Asteroid Surface Scout (MASCOT) which is in fact small jumping multifunctional probe.

Fig10. Asteroid mission timelines: Hayabusa2 and OSiRIS-REx. Credit: University of Arizona.
(https://www.asteroidmission.org/?attachment_id=6649)

The German Aerospace Center (Das Deutsche Zentrum für Luft- und Raumfahrt) developed MASCOT for MarcoPolo ESA mission with contributions from the French Centre National d'Études Spatiales. Battery power supplied rover has a camera, a radiometer, a magnetometer, a hyperspectral microscope, and other instruments. They allow for a short time (16h) investigations of regolith thermal, textural, size properties, temperature changes during a rotation cycle, global/local magnetic fields, surface materials mineralogy, organic and other substances' detection [23-25].

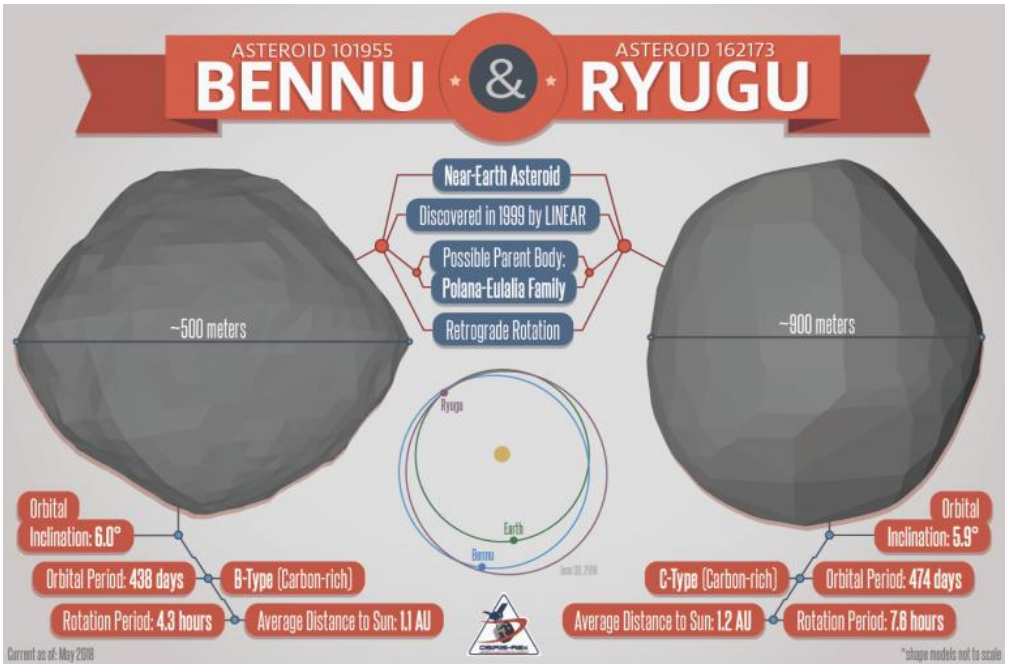

Fig.11. Asteroid comparison: Ryugu and Bennu.
Credit: University of Arizona.
(https://www.asteroidmission.org/?attachment_id=6650)

Some of Ryugu's and Bennu's parameters are very similar (fig.11). Ryugu's 474-day orbit with semi-major axis of1.2 A.U. and eccentricity of 0.19 is 5.9º inclined to the ecliptic. The perihelion and aphelion are 0.96 and 1.41A.U so the orbit of the asteroid comes close to the orbits of Earth and Mars. The asteroid closely encounters Earth every thirteen's year after ten orbital revolutions. The minimal distance between 900m wide slow retrograde rotator Ryugu and the Earth is around a quarter of lunar distance i.e. around hundred thousand kilometers. Groundwork shape model of Ryugu based on the inversion of two maxima optical and thermal infrared lightcurve data was given in [26]. The model looked roughly spherical there. We know nothing about detailed radar observations of the asteroid.

Ryugu is a dark near-Earth asteroid of C-type alike carbonaceous chondrites. To be more exact it belongs to rare spectral subtype Cg, with the properties of both C and G asteroids. Spectral observations indicate iron-bearing phyllosilicates on some surface areas [27]. C-type and its relative B-type asteroids (e.g. Bennu) are thought of as the most primitive bodies in the inner Solar System. They are believed to be rich in volatile materials incl. water and organics. Thus the search of life precursors is one of the conceptive foundations of the missions together with the prevention of virtual asteroid hazards to Earth and deciphering evolution of the Solar System.

4.2 Diamond-like shape of Ryugu

To be aware of the contemporary situation with asteroid shape predictions our readers are recommended to visit Hayabusa2 mission's page dated on 5 June 2018 where tens "project members and professional creators take a guess about what Ryugu might look like", given the above spherical model was known to them (http://www.hayabusa2.jaxa.jp/topics/20180626_e/index_e.html). It is impossible to find there anything in common with the shape discovered this June when Hayabusa2 arrived at the asteroid.

Side views of Ryugu turned out to be rhomb-square ones (fig.12). The asteroid was found to have diamond-like appearance of the asteroids discussed above and repeats even details of their reliefs. It has "very circular equatorial bulge" (pg.23 [30]). Brilliant shape of the spinning top seems to make Ryugu the larger sibling of Bennu.

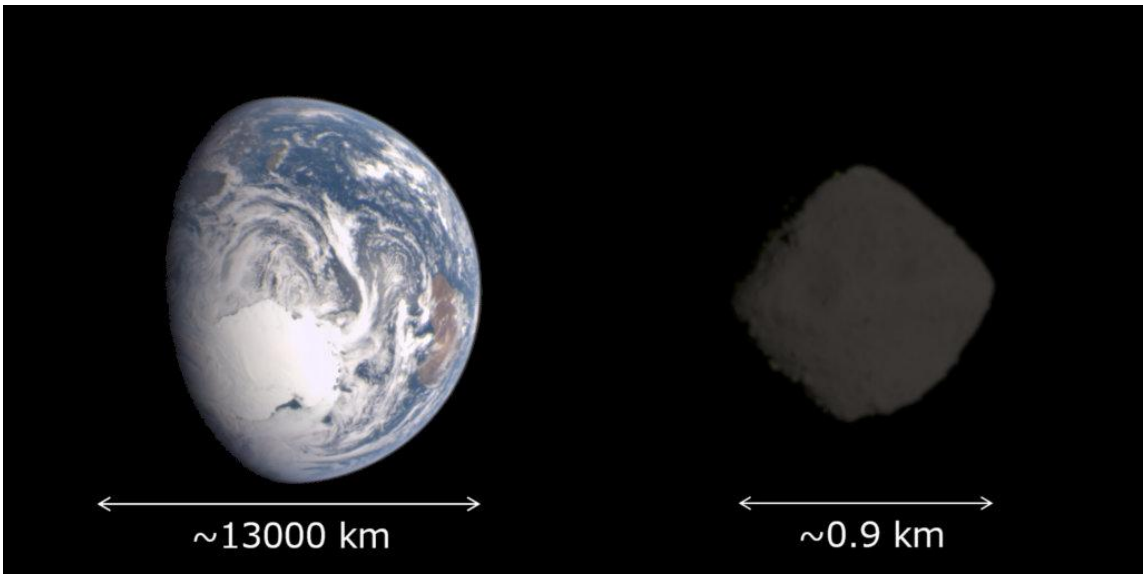

Fig.12. Earth's and Ryugu's views, taken with the same Optical Navigation Camera - Telescopic (ONC-T) camera of Hayabusa2 probe. The natural color of the dark asteroid was created from the multiband image (0.48, 0.55, 0.70 microns wavelengths).
Image credit: JAXA. Uni.of Tokyo & collaborators.
*(*http://www.hayabusa2.jaxa.jp/topics/20180629je/index_e.html}

Now new data on Ryugu are regularly supplied by JAXA (www.hayabusa2.jaxa.jp). Excellent work of Hayabusa2 team allows see all sides during Ryugu's comparatively slow (7.6h) rotation cycle, except for two polar views yet. The comment to the high resolution image shown in fig.13 states that "this form of Ryugu is scientifically surprising…" Contrary, in the frames of our ejective approach the shape of Ryugu is hardly surprising, being natural and typical amongst many other asteroids.

As for Ryugu's origination it is analogous to Steins (see fig.4). The apex angles of two base contacting cones which comprise the asteroid shape are close to 90º. One apex was determined by parent repose angle, another – by parent crustal tensile/shear strain trade-off. The general symmetry of Ryugu is the axial one and the axis is perpendicular to the orbital plane. The awaited northern views may demonstrate curved spiral prone relief features.

4.3 Global views and features

Our rationale states that necessary asteroid formation condition is the fault crustal development with simultaneous crack opening, local plasticity evolvement, and dyke or streaks originations as the means to alleviate mechanical stresses in the fractured areas. To prove that we further describe the morphology and relief features of Ryugu from larger to smaller scales with simultaneous explanations.

Detailed pictures are not always necessary for history and global relief analysis. For example vague image in fig.13 (right) allows discern interrelations of large scale relief features and huge southern crater. Another big crater is seen on the ridge. It is the largest of Ryugu's crater about 200m in size with angular rhomb-like perimeter. There is an elevation tens meters in dimension between the craters. It seems to be crossed by the vague dark depression stripe (fig.13 long arrow).

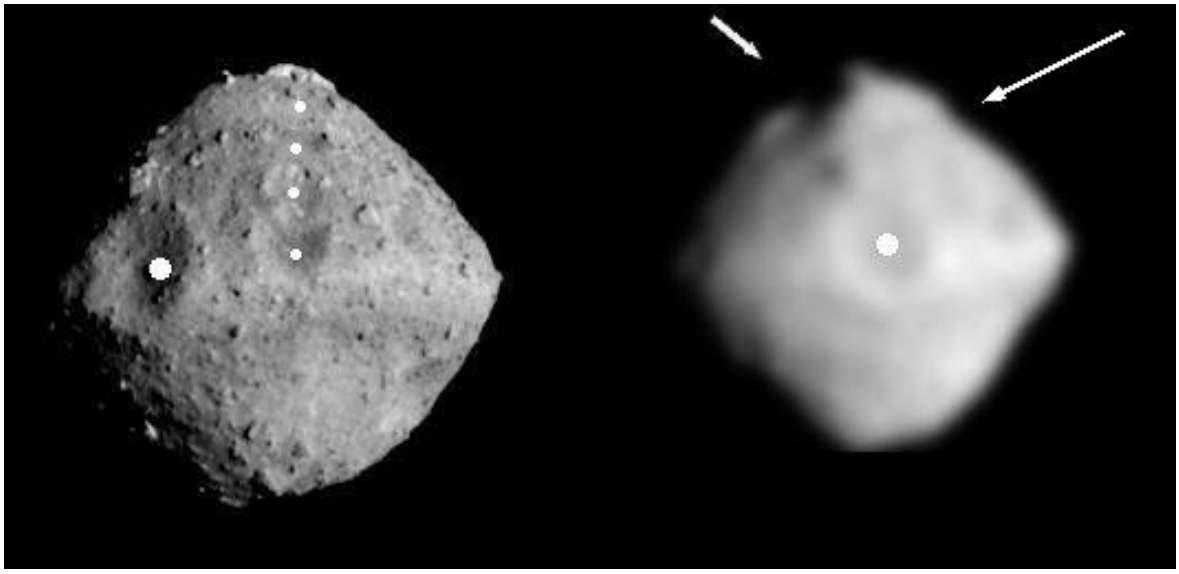

Fig.13. ONC-T images of Ryugu acquired on 24 (left) and 17 (right) June 2018 from distances 40 and 245km, respectively. Light and dark regions of the right image are emphasized with the squared brightness. Long arrow directs dark lined depression (see text), short arrow points to remains of large southern crater. The largest ridge crater is marked with thick dots. Catena is punctuated with small white dots. Its fracture is seen to continue directly to North apex and is revealed by relief elevations. The South is up.
Image: credit: JAXA. Uni.of Tokyo & collaborators.
(http://www.hayabusa2.jaxa.jp/topics/20180625je/index_e.html)
(http://www.hayabusa2.jaxa.jp/topics/20180619je/index_e.html)

Side views of the rotating asteroid are shown in fig.14. According to JAXA press releases the most prominent feature of Ryugu is its angular equatorial bulge. The ridge is averagely stronger and slightly brighter than its surroundings due to plastic compositional modifications (see also map in fig.15). The ridge is really strong equatorial mountain range laced with craters, the rhombic largest one being located 90º longitude. The crater is situated in the asteroid singular region of the highest plastic changes that is in the vicinity of the global fault (see [6.7]).

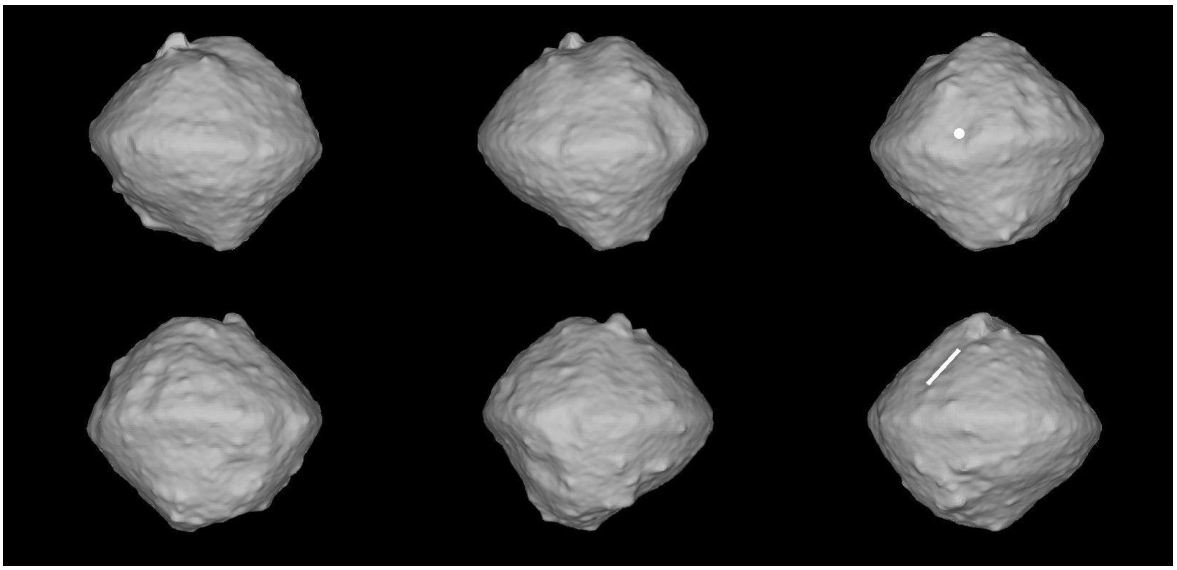

Fig.14. Haybusa2 views of rotating asteroid Ryugu. The South is up. Six views were extracted from the model image of Ryugu presented by the University of Aizu as gif format file. Angles between the views are 60º. Views of upper row are in opposition to those of lower row. White point marks the largest rhomb ridge crater, line covers part of global fault remnant groove approximately opposite to the crater. Notice zigzag elevations in the northern cone of the lower right view. Image credit: JAXA. Uni.of Tokyo & collaborators. (http://www.hayabusa2.jaxa.jp/topics/20180711bje/index_e.html)

The first map of asteroid Ryugu is presented in fig. 15. It also shows plausible landing sites which were actively studied by the mission team.

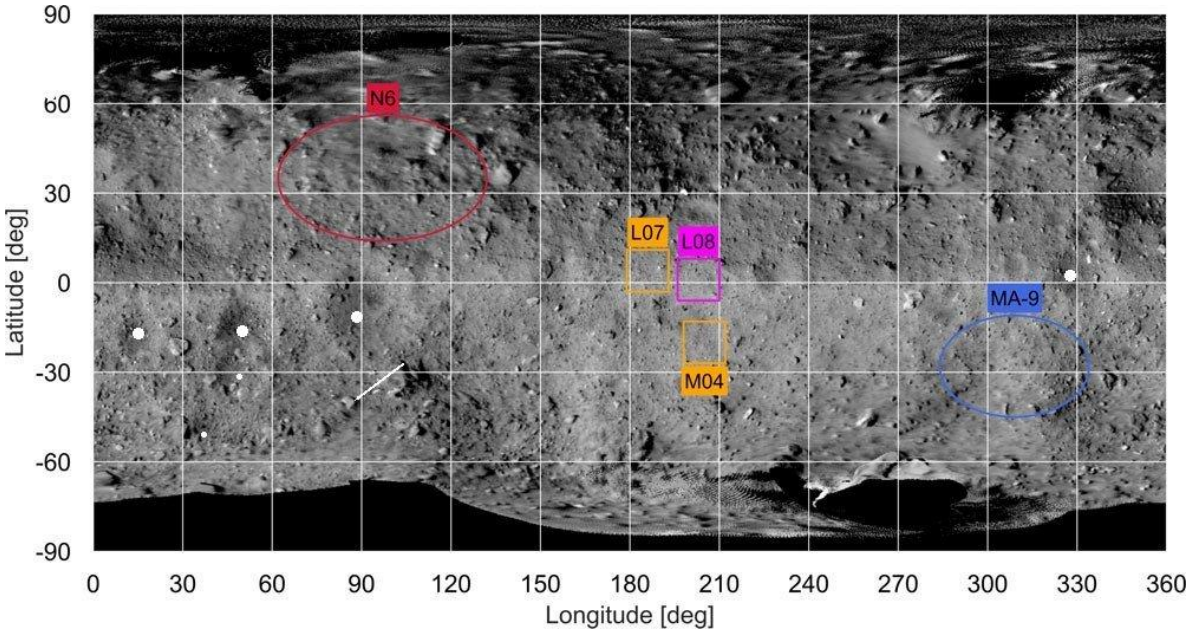

Fig.15. Relief map of Ryugu with marked plausible touchdown equatorial area (near L08) and expected landing sites for MINERVAs and MASCOT. The North is up. Big spots mark equatorial craters, small spots mark catena (cf. fig.13). Line directs fault remnant which crosses the brighter rock pile near the largest crater. Image credit: JAXA. Uni.of Tokyo & collaborators. . (http://www.hayabusa2.jaxa.jp/topics/20180829/img/fig1.jpg)

We marked the centers of dark crater regions along the equatorial bulge with thick spots in fig.15. Those approximately regular craters appear to be the remains of regular dykes or streaks formed inside parental crust (see also [7]). Unmarked side (approx. 160°-310° longitudes) also contains smaller equatorial craters. This implies differences in crater statistics in different surface areas of Ryugu as is the case for Steins. One side of Ryugu is separated from another side by the groove remnants of the global fault (e.g. fig.14). The crescent of the global fault groove that was partly marked in fig.14 with white line crosses the equator near blue rectangle (310° longitude) in fig.15.

Greenish and reddish colors of stereo views are helpful for analyzing large scale morphology divisions of Ryugu. Nine stereo images of fig.16 support the conclusion that it consists of several large blocks separated by inner faults.

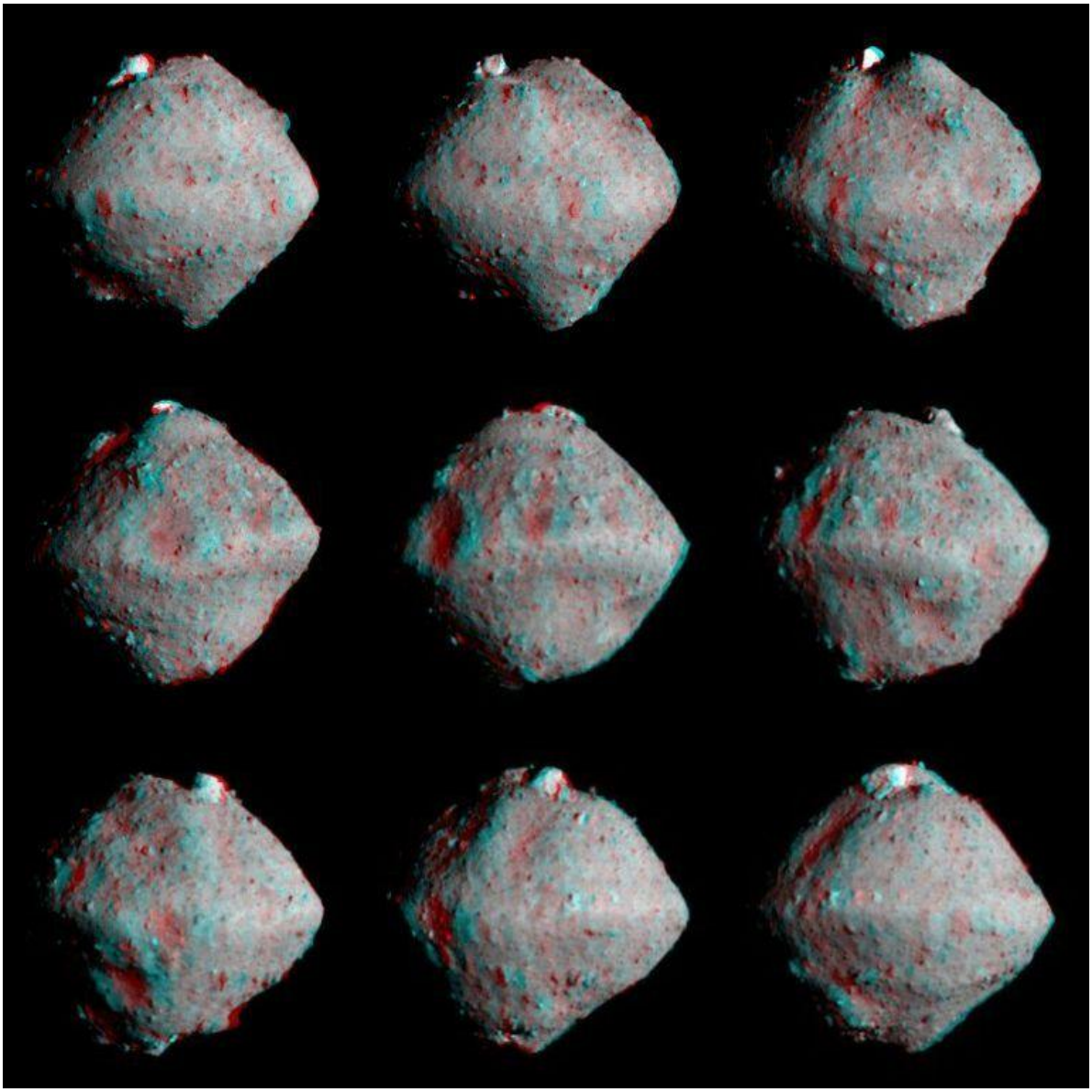

Fig.16. Stereoscopic views of Ryugu extracted from its full rotation animation (gif format file). Views were captured by ONC-T on 23 June 2018 from 40km altitude. When viewed through red/blue (left/right eye) glasses the views are 3-D. Image credit: JAXA. Uni.of Tokyo & collaborators. (http://www.hayabusa2.jaxa.jp/topics/20180710je/index_e.html)

In upper right corner image of fig.16 two roof side blocks crowned with white boulder look like remnants of crustal shells above the asteroid body. The view is one of the evidences of plastic reshaping and growth of the asteroid due to its inner stresses. Other evidences are red/blue lines conically crossing in the southern half of Ryugu shown in upper left image of fig.16. Jointly lines form roof-like angles with sides parallel to the asteroid ones.

Ryugu consists of two lobes. The smaller lobe is clearly seen separated from the larger one by the global fault groove. The lobe is shown almost face-on in the lower right image of fig.16. The separating crescent is clearly masked with reddish stripe in fig.17 (right). The opposite view with pointed centers of the largest crater and the region of the same size is also shown in fig.17 (left). The suspicious region is encircled with a handful of boulders and highlighted with greenish color.

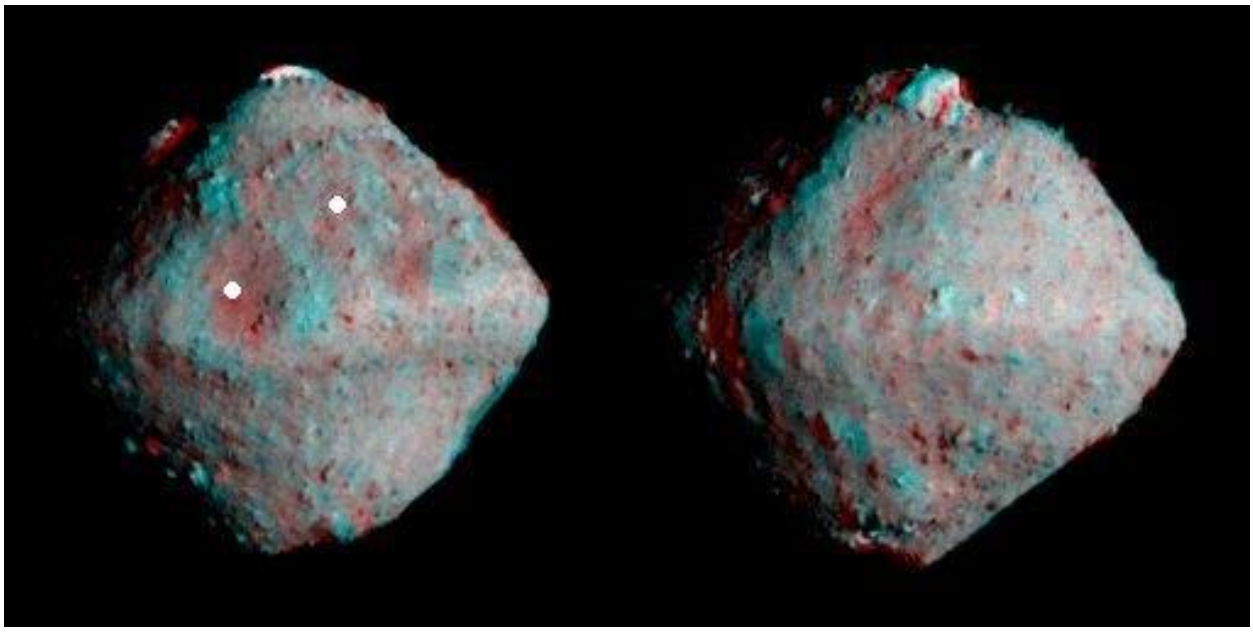

Fig.17. Two opposite views of fig.16. Centers of similar sized relief features are marked with white dots.
Image credit: JAXA. Uni.of Tokyo & collaborators.
(http://www.hayabusa2.jaxa.jp/topics/20180710je/index_e.html)

In the process of explosive ejection rotational forces are exerted on the lower (northern) part of the asteroid as a result of curved dyke movement. The rotation of the upper (outer) part is accelerated by the lower one and lags behind it due to inertia. That is why differential rotation stress along symmetry axis exists at the start. The torsion reveals in surface triangle and rhombic features (fig.18). The same reasons, for instance, appear to determine the angle between catena direction and apex-to-apex line (e.g. fig.13). Generally, the large scale relief reflects initial stages of plastic evolution of newly ejected solid body.

Similar but a bit different perspectives allow for effective feature comparisons (fig.18). Pay notice to border geometry of dot marked depression and color revealed parallel relief lines to the left of its leftist border. The depression resembles the rhomb-like pit of Steins shown in fig.3 (left). The ripples are to the places of upper crust sliding in the plane perpendicular to the asteroid surface and of lined distributions of different substances and minerals.

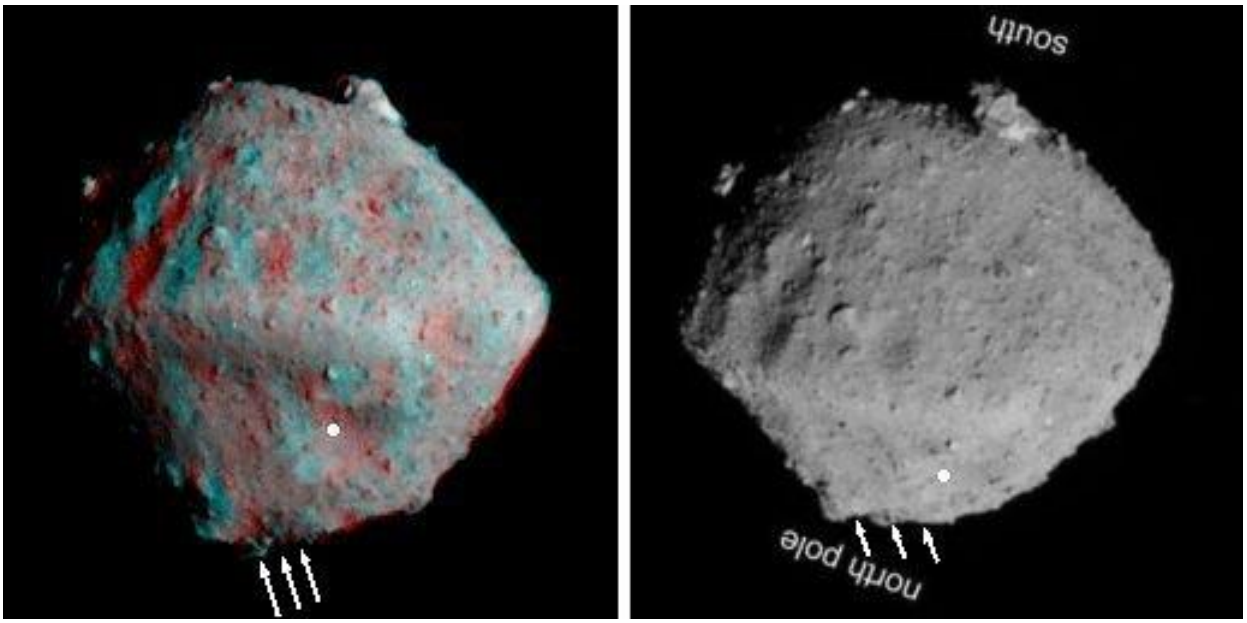

Fig.18. Left: Middle row right view from fig.16. Right: Image captured on 24-08-2018 with ONC-T 9km above Ryugu's equatorial plane from altitude 22km. (pg.9 in [31]). It was rotated by us. Dots mark angular depression, arrows point to rippling relief lines parallel to its margin.
Image credit: JAXA. Uni.of Tokyo & collaborators.

The system of global lineaments is oriented in North-South, East-West directions and 45° to them. The tension/shear stress symmetry embraces all dimensions. Ryugu's relief features down to minute surface boulders look angular, kinked, and wedged. The reasons are that surface crustal layers are geologically fresh and are still under the influence of inner stresses. Recent publication of thermal and spectral maps of Ryugu proves this approach.

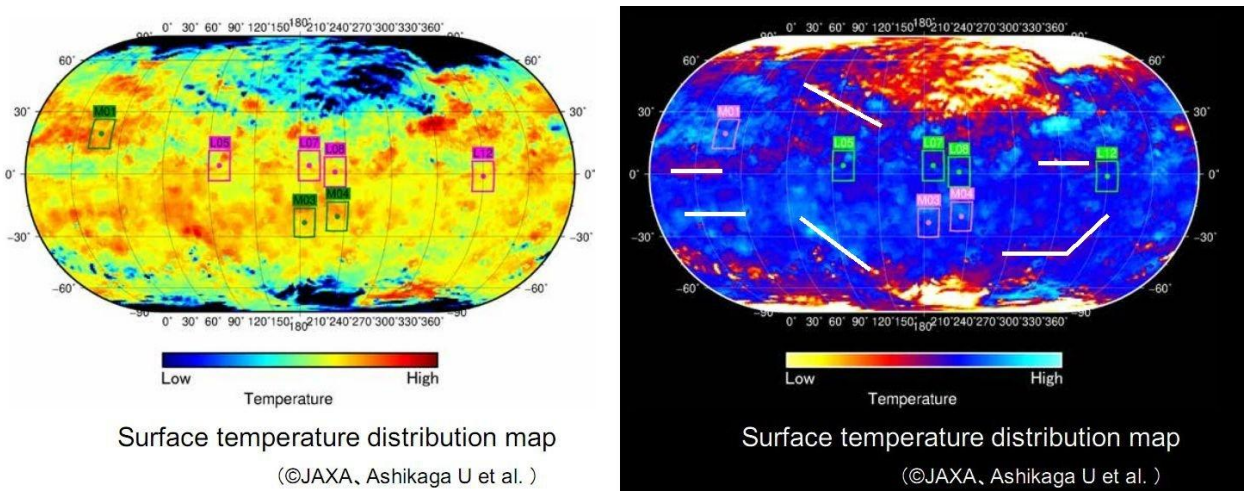

Fig.19. Left: Map of Ryugu's surface temperature distribution (pg.19 in [30]). The same color inverted map is given (right) to make the symmetry of global temperature distribution more discernable. Some large scale temperature features are marked with white lines. For detailed feature comparisons it is advised to invert colors of the figure.
Image credit: JAXA. Uni.of Tokyo & collaborators.

Spectral map data on the asteroid surface examined with optical navigation camera of Hayabusa2 spacecraft are presented on fig.20.

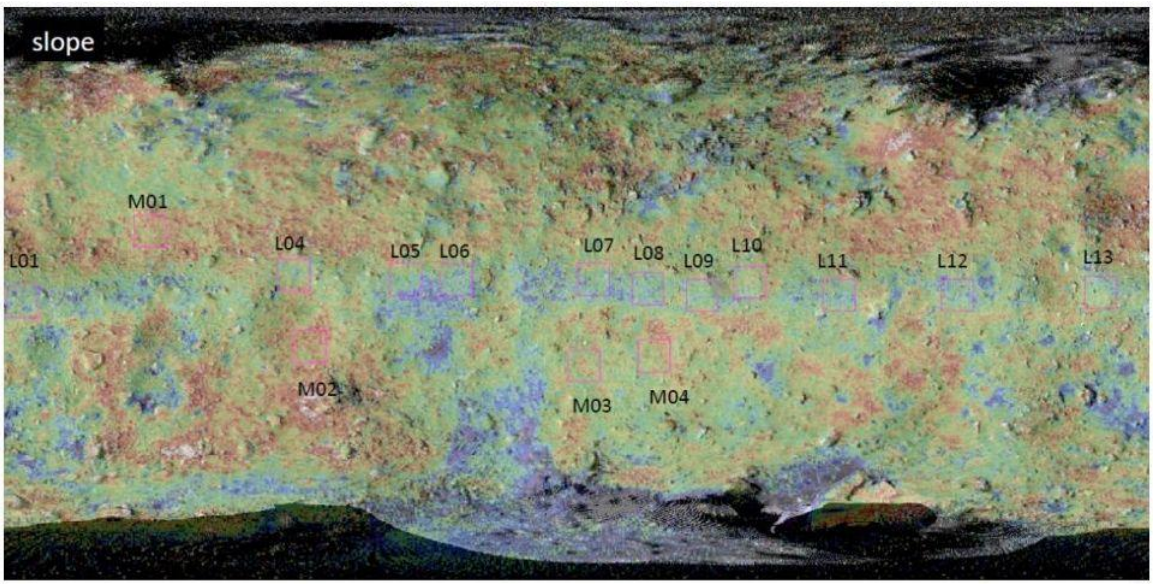

Fig.20. Map of spectral slopes of Ryugu acquired with ONC-T camera in the process of scientific evaluation of the landing site candidates. No more details are given in JAXA's press release (pg.25 in [30]). The North is up.
Image credit: JAXA. Uni.of Tokyo & collaborators.

The equatorial ridge revealed with bluish colors seems in average to be covered with substances younger than those of other areas. The same holds for craters. The largest ridge crater looks averagely redder i.e. older than others and its rhombic symmetry is also color revealed. Crescent main fault remnants are color marked that proves plastic renewal of these areas. Whiter map colors mark surface boulders which appear to be the youngest relief features implying quick crater planarization due to inner plasticity and regolith coverage. The South–North dichotomy is obvious. Southern polar areas are violet that proves their younger ages and prevailing regional geologic activity.

4.4 Local relief features

Angular boulders of different sizes are dispersed all over the asteroid surface. There is cliff-like whitest Ryugu's boulder of triangular geometry in the southern polar region (fig.21). It is approximately hundred and half meters in size and has the brightest colors of highly reflective body (e.g. fig.17). That is the sign of its freshness which is natural for other asteroids. The asteroid polar views are to prove the existence of crater-like depression of similar size somewhere near the boulder (see later fig.24).

Fig.21. Left: Ryugu's image acquired from a distance of 20km on 30 June 2018. Right: a crop from left image with the bright angular boulder (cf. figs. 16, 17). Image credit: JAXA. Uni.of Tokyo & collaborators. http://www.hayabusa2.jaxa.jp/topics/20180711je/index_e.html

Large angular faceted rocks, their groups, angular boulders are everywhere but their positions are not chaotic and reflect discussed shear/tension symmetries. In some places they appear to be accompanied by obscure pits and depressions of approximately same sizes. That mass lack of apparent craters may be explained by their plastic healing due to activation of substance diffusions in the bulk of Ryugu. The examples of relief local changes, growth, crater and crack healing for shorter timescales were observed by ESA's Rosetta probe on comet 67P/Chury [32].

Another example of young relief features is the angular boulder pile-up near the largest ridge crater (fig.22) Triangular parts of the pile are brighter than average but not as white as the southern boulder. Brighter boulders due to their freshness are going to be more helpful for the search of coincident craters. The younger they are, the more vivid are to be nearby depressions of similar geometries.

Fig.22 is as well the evidence of shear stress prevalence near the largest crater in equatorial area. Shears are clearly delineated by boulder arrays in the lower part of the figure. According to JAXA's press release (pg.26 in [30]) mid-latitudes seem to have many smaller sized particles. We think the effect may result from stronger than average rock substances that comprise the bulge. They in turn appear to be formed due to highest ridge plastic reshaping while Ryugu's origination

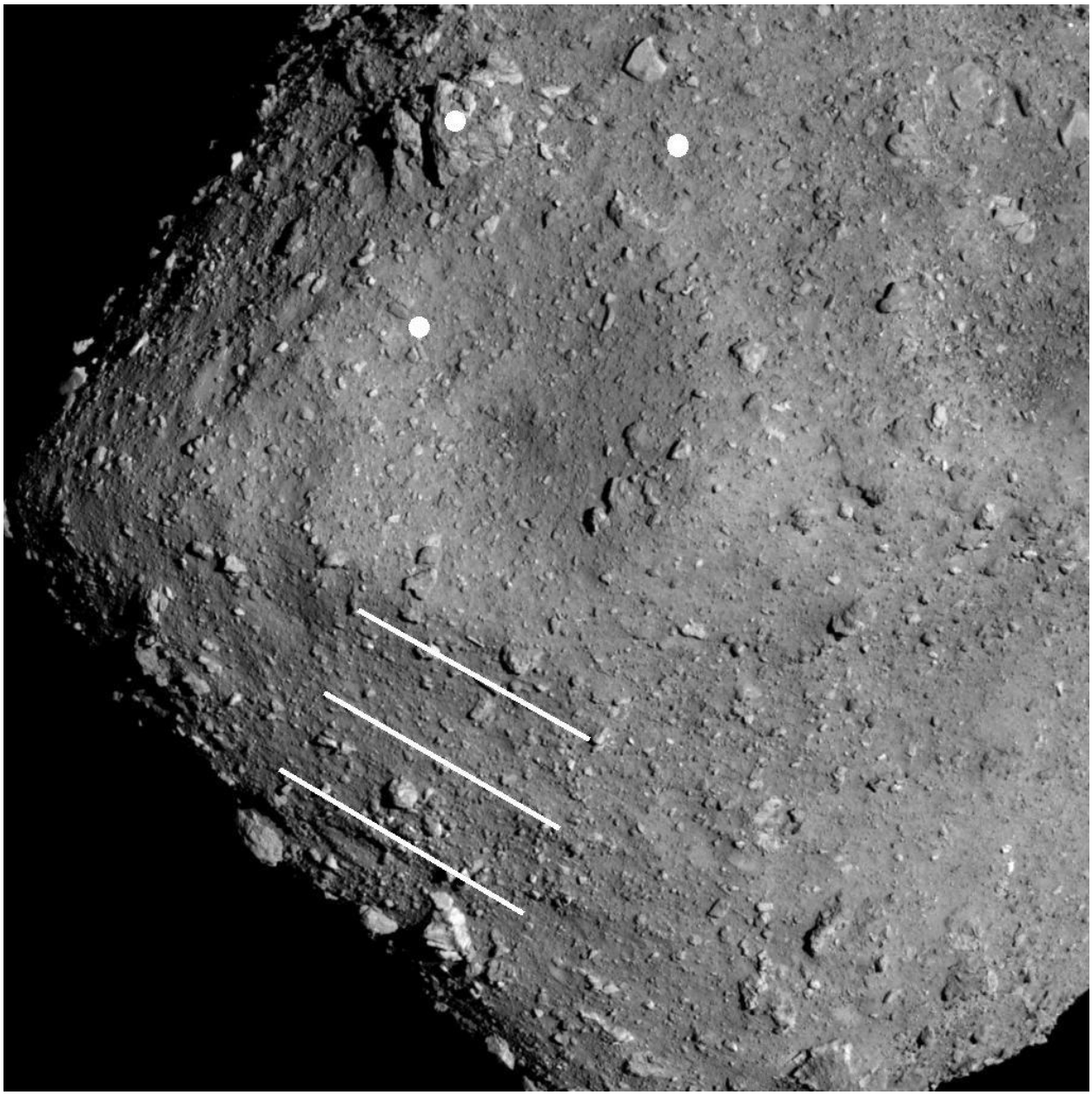

Fig.22. Ryugu's ONC-T image acquired on 20 July 2018 from an altitude of 6km. Centers of angular boulder pile-up and of the nearest same-size rhombic features are marked with white dots. Lines show direction of shears.
Image credit: JAXA. Uni.of Tokyo & collaborators.
(http://www.hayabusa2.jaxa.jp/topics/20180725je/index_e.html)

Hayabusa2 team found that the number of boulders per unit area greatly varies over the surface of Ryugu. Fig. 23 clearly proves the conclusion. To be exact we cite descriptions of original images. Right image of the figure "shows the region of Ryugu's surface where the boulder coverage is comparatively low". Left image "shows a region where there seems to be far more boulders (although it is possible that this will change with more detailed analysis in the future). Both regions have hundreds of identified boulders, but there is also considerable variation between places where the boulder number is particularly high and regions where there are fewer."

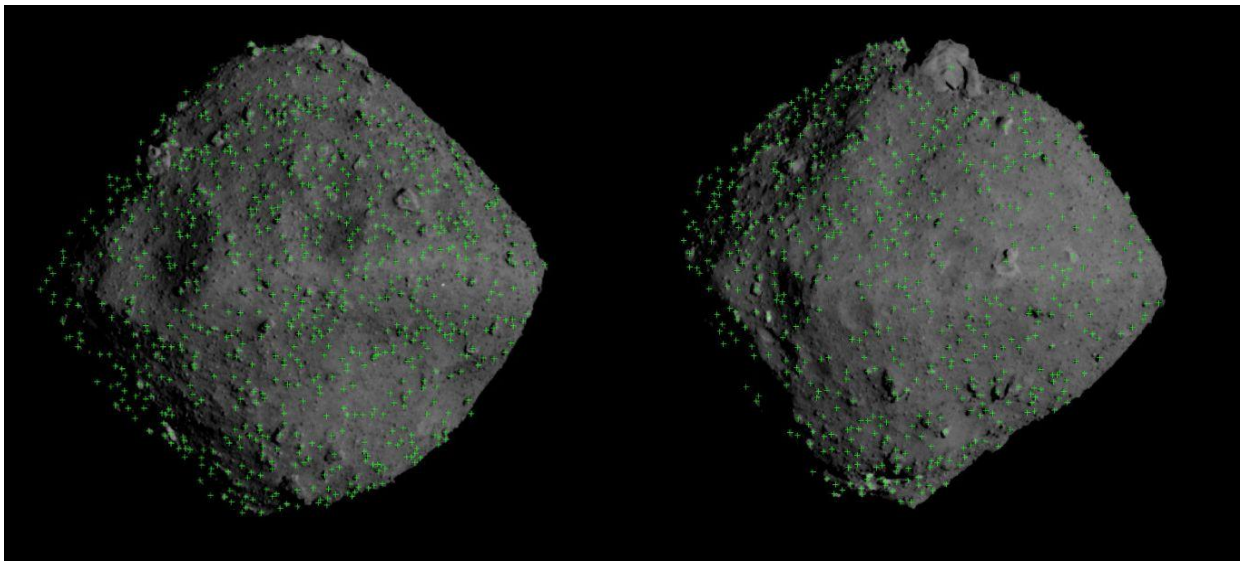

Fig.23. Boulder distribution on Ryugu's surface. Views are centered at 60° (left) and 300° (right) longitudes. According to original description green marks point boulders "between 8m to 10m and more." The South is up.
Image credit: JAXA. Uni.of Tokyo & collaborators.
(http://www.hayabusa2.jaxa.jp/en/topics/20180906e/)

The viewer is recommended to invert colors of fig.23 to discern surface symmetries and features delineated with laces or throngs of green marks turned pink. Distinguish color highlighted groove that separates Ryugu's lobes which host different boulder concentrations and, according to our rationale, concomitant different crater concentrations. It is interesting to note that different magnifications reveal different symmetries of features.

With the help of laser location (LIDAR equipment) a handful of crater profiles were measured. It was found that their depth to diameter ratios are 0.1-0.2 and "there appear to be craters with relatively clear edges (about 5m high?)" [pg.9 in [29]). The ratio is normal for asteroid and comets. The protruding edges are also not unusual for asteroids.

To our opinion crater small depth to diameter ratio is due to their healing in the course Ryugu's plastic evolution. High efficiency of the evolutionary processes on the small celestial body may explain lack of small craters on the surface of Ryugu. Clear outer crater edges result from severe border plastic modifications during explosive orogenesis. The whole asteroid surface gives the impression of interrelations of large scale plasticity and small scale ejections. Average dimensions of relief features equal to their depths. That means ejective orogenesis is active in surface and subsurface crustal layers. The conclusion is consistent with current evolution tranquility of the Solar system.

We magnified several areas of fig.23. In fig.24 parts of it are cropped to detect characteristic, curious, and weird features of the asteroid. For instance, long almost vertical white line in the leftist image outlines straight boulder lace that marks border of the largest Ryugu's catena (see e.g. fig. 13). The narrow white line that crosses the vertical one discloses inner crustal fracture approximately parallel to the equator. There are lots of shorter boulder laces parallel to both white lines. Their existence means sliced-like evolutional expansion of the asteroid. This evolvement is similar to Earth's transform faults (fracture zones) oriented at right angles to Mid-ocean ridges.

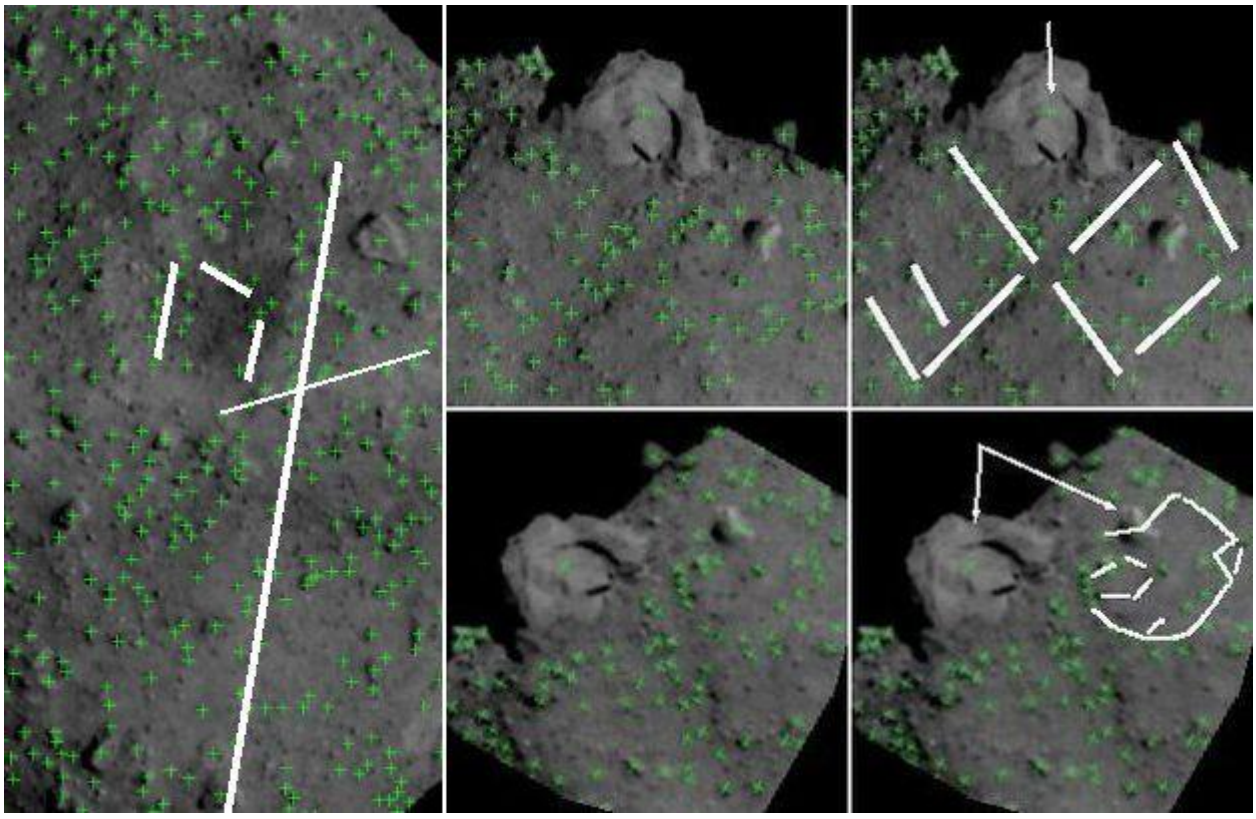

Fig.24. Marked crops from fig.23. The leftist view is crop of fig.23 (left). Middle column upper image is cropped from fig.23 (right), lower column image is the rotated upper one. Right column is the marked middle column images. See text for explanations.

Boulder mark groups reveal rhombic structures inside the main crater of the catena in fig.24 (left). These marks are parallel to the crater boundaries. There are similar structures inside the largest ridge crater. They are crossings of crater surfaces with horizontal crustal layers of Ryugu. It is those layers the thickness of which determines their instability wavelength and in the final run sizes of craters in them. Rhombic structures of similar size are demarcated in the southern polar region with same white lines (fig.24 upper right image). They prove the existence of same crustal layers in southern half of the asteroid. The largest Ryugu's boulder is similar in size to the nearby white marked rhombs.

The lower right image of fig.24 shows rotated polar view with the relief features which seems to be topologically analogous. The mirror of their symmetry is approx. the plain of the main Ryugu's fault. The polygonal feature appears to be the place of the southern boulder origin and the remnant of concomitant crater depression. Two arrows point to smaller boulder crossed by the marked crater perimeter and same size cavity on the surface of the largest boulder. The situation needs further scrutiny, especially spectral one.

The arrow in the (fig.24 upper right image) points to a green mark of a boulder on the surface of order of magnitude larger one. Green mark is located near dark stress concentrating crack of the largest southern boulder. The crack appears to be the reason of the marked boulder origination. The situation is similar to the bizarre boulder on central cliff peak of lunar Tycho crater.

4.5 Landing and touchdown areas

In preparation to landings and touchdowns the asteroid equatorial region was studied by Hayabusa2 team. Fig.25 presents three side views of Ryugu.

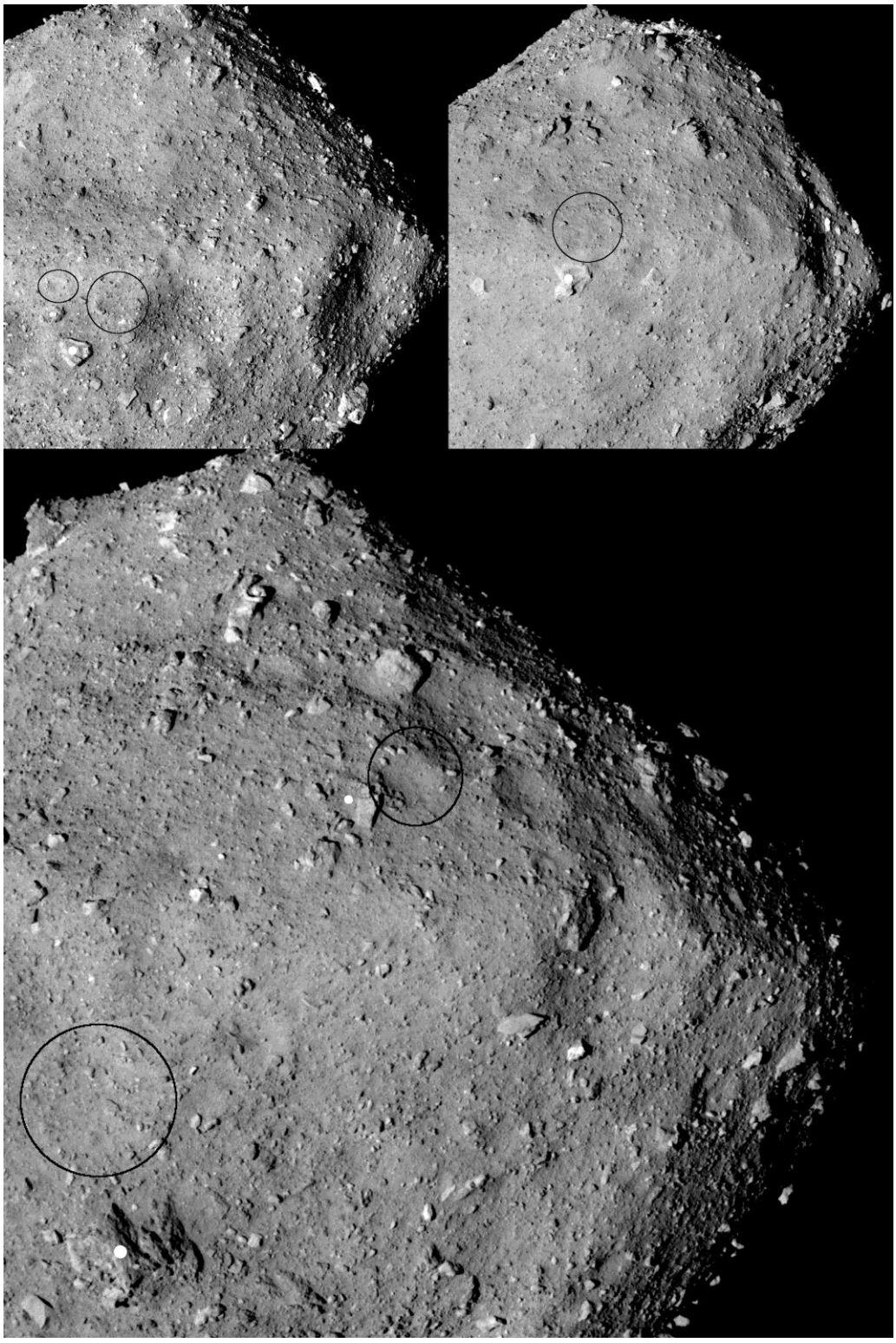

Fig.25. Three side views of Ryugu. Circles mark depressions geometrically coincident with dot marked boulders down or down left to them. The North is up. Image credit: JAXA. Uni.of Tokyo & collaborators.
(http://www.hayabusa2.jaxa.jp/en/topics/20180905e/)

In fig.25 we encircled some topologically similar surface depressions and supposedly concomitant elevations. Exact geometrical analysis of them is time consuming and requires detailed images from different positions. Thorough investigation of the questions is impossible without local color and spectral information. We are seeing forward the detailed analysis of high-resolution pictures and local mineralogy.

Similar size elevation (black circle) and depressions (white circles) were also found close to color marked areas of future Hayabusa2 touchdown (fig.26). Our feeling is that the lower circle area in the figure was the right place for the crossly destructed boulder to be brought about. The ability to closely explore the region of interest will be of great help to solve the problem.

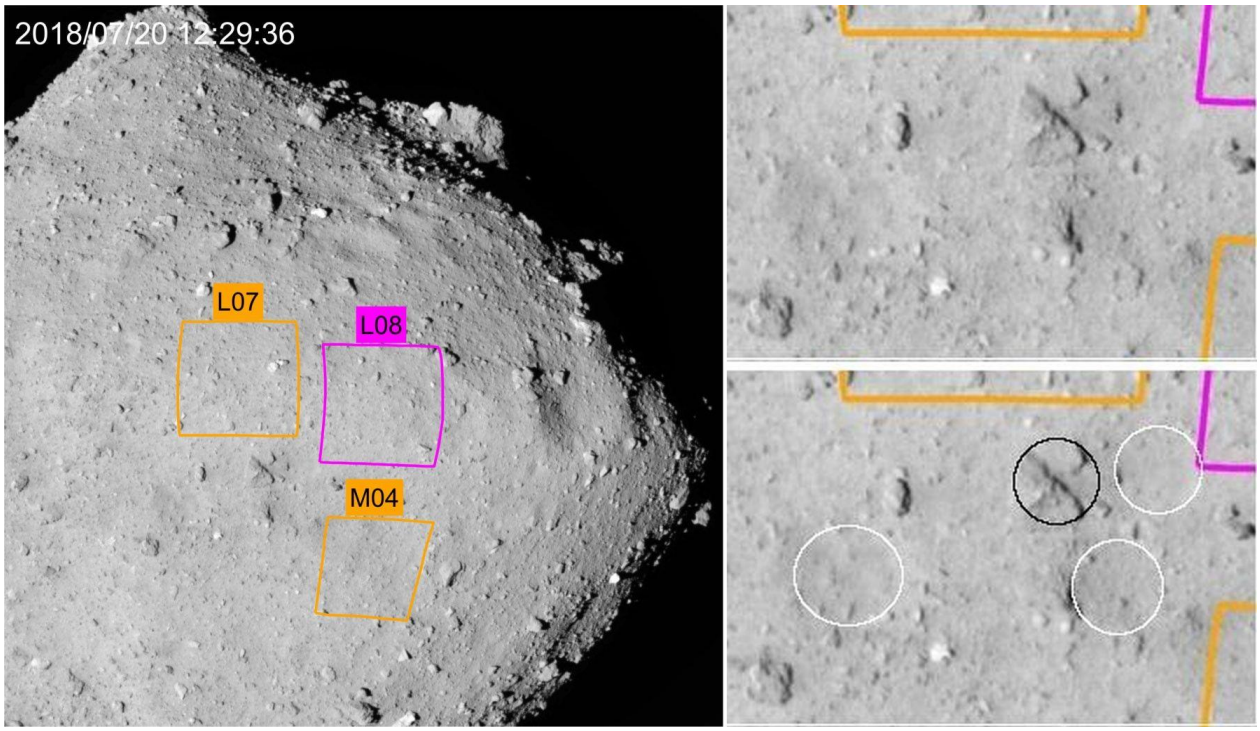

Fig.26. Left: Ryugu's image with plausible touchdown and landing places. Right up: The crop from left image. Right down: The same crop with encircled destructed angular boulder (black) and encircled depressions of similar sizes (white). The encircled areas are angular shaped.
Image credit: JAXA. Uni.of Tokyo & collaborators.
(http://www.hayabusa2.jaxa.jp/topics/20180829/index.html)

All discussed above relief features are possible to be studied by Hayabusa2 instruments. Optical, radar, thermal, and infrared sensors of the probe will permit their comparisons and coincidence determinations. According to our rationale the most active areas are to be the vicinities of craters and linear features (fractures, faults). They are possible to produce higher magnetic fields, dust, and gas exhaust which may be synchronized with rotation cycle due to nonlinear interactions of rotation and oscillation eigenmodes of Ryugu.

On smaller scales Ryugu's relief features still save the symmetry determined by inner stresses. In those cases the thinner crustal layers produce superposition of periodic relief structures and pile-ups. We revealed them by digital shadowing of touchdown region in fig.27. Different shadowing exposes different surface ripple gratings, opposite shadowing – same gratings.

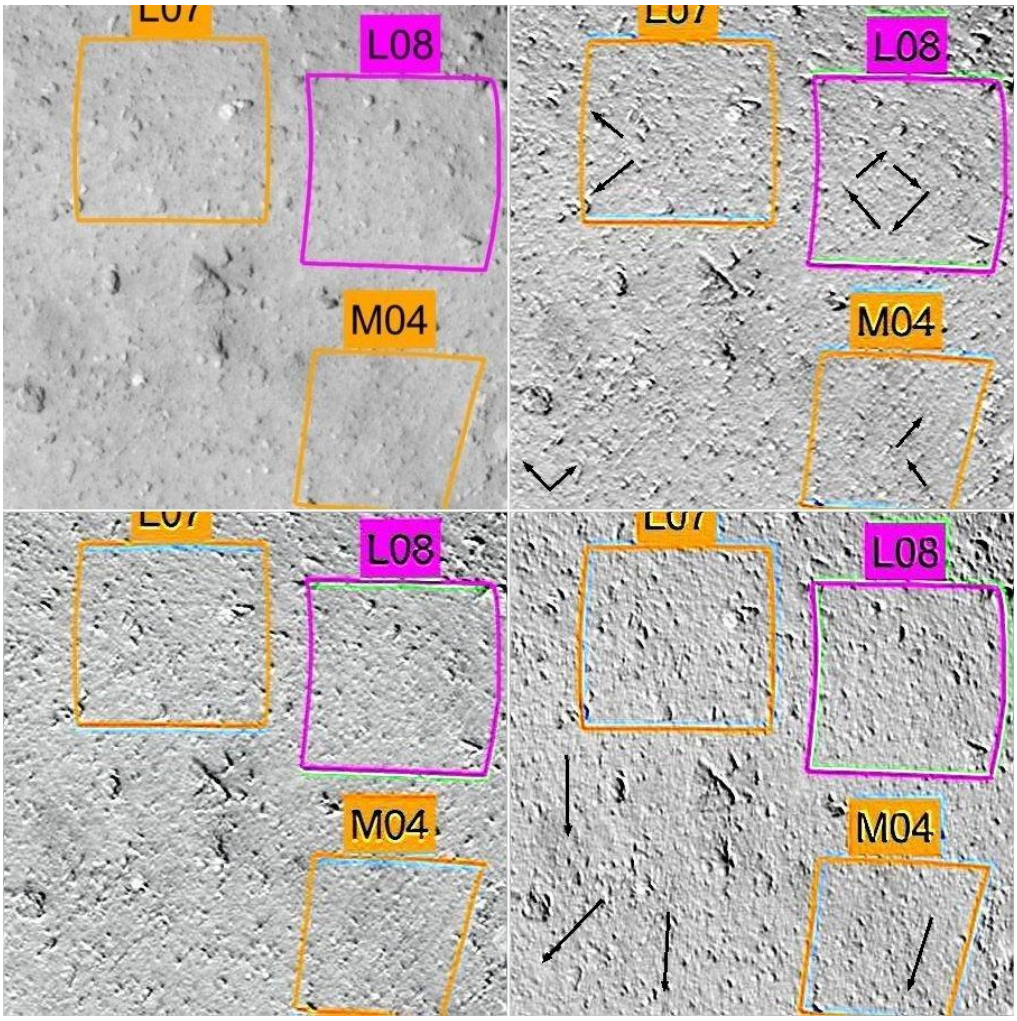

Fig.27. Upper left: Central part of fig.26. From upper right clockwise: three digitally shadowed central views. The shadows are directed: North, North-East, and South. The directions are easy to determine by color shadows of color rectangles' borders. Black arrows show some surface grating directions revealed by shadowing. Opposite shadowing reveals same pictures (upper right versus .lower left images). Color inversion is recommended to discern details.
Image credit: JAXA. Uni.of Tokyo & collaborators.

Organic materials on other asteroids are located in patches with high concentrations, for instance, on Ceres [33]. Authors think that if organics is produced or preserved locally and there should be some mechanism to concentrate it. Our explanation is that organic materials were synthesized in the course of explosive ejective orogenesis. Thus we anticipate the same situation with Ryugu and other asteroids. Besides, different substances on the surfaces are to reveal crustal lineaments as it is for phyllosilicates on Ceres [34] (cf.fig.20). Some minerals of Ryugu are to be magnetic.

Different transients, e.g. splashes, auroras, minor ejections are possible to happen above discussed locations because Ryugu is by no means a pile of independent parts, boulders, or planetesimals. It is a unique integral celestial body of its kind with nonlinear interconnections of its constituents and with diverse feedback loops still unclear to us. Electromagnetic fields of the asteroid may unpredictably change while close approaches and impact experiments. The first touchdown rehearsal LIDAR failure may be connected to them.

5 Parameters and properties of Bennu

5.1 General pre-encounter data

Now we consider distant astrophysical data on near-Earth asteroid (101955) Bennu. Observers acquired its size, albedo, photometric constraints, spectra, orbital characteristics, etc. They even discerned some relief details. Theorists estimated Bennu's density, shape, and other parameters on the basis of contemporary knowledge about asteroids. All the data are systematically reviewed in [1-4].

Bennu was found to be 0.5km in diameter carbonaceous B-type asteroid with featureless spectrum, slightly bluish in the visible range of wavelengths, minute reddening in the infrared, and minor ultraviolet drop off. It resembles carbonaceous chondrite meteorites. To recollect, chondrules are believed to be lava droplets of silicate magmas. The asteroid has very dark visible geometric albedo 4.5% (percentage of reflected light). For human eyes the asteroid would look like charcoal chunk. No satellites larger than 15m were radar found around Bennu.

The retrograde rotator's orbit together with orbits of inner Solar System planets are shown in fig.28 (see also fig.11). Bennu's rotation axis is approximately perpendicular to its orbital plain, the axial tilt is around 176°. With the eccentricity equals 0.2, the aphelion - 1.36 A.U., perihelion - 0.90 A.U., and semi-major axis – 1.13 A.U., the orbital path comes close to Martian orbit and almost crosses that of the Earth. The orbital plane is slightly inclined to ecliptic (6°) and the revolution period is one fifth larger than a year (436.65d). That means the asteroid is in quasi-resonance with the Earth and every six's year returns to closest encounter with it.

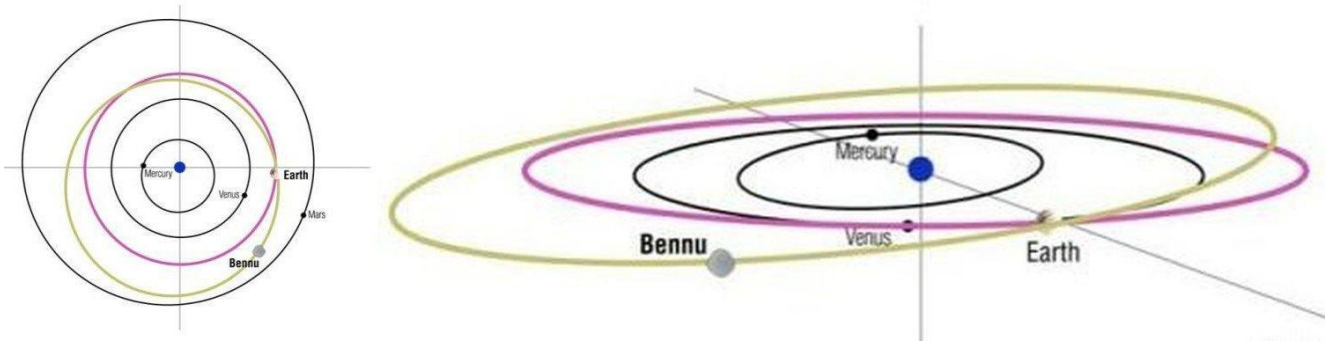

Fig.28. Orbits of Mercury, Venus, Mars (black), Earth (purple), and Bennu (greenish yellow) on approach phase time 21-09-2018. Bennu's plane of revolution is inclined 6° relative to the ecliptic. Its rotational axis (z axis) is directed along the solar northern pole, an axis marks vernal equinox. The image made use of color inverted figure 7 from [1].

The analysis of Bennu's astrometry for 14 years (1999-2013) allowed determine the drift of its semi-major axis due to deviation from purely gravitational dynamics (284m per year). It is commonly thought to be the result of Yarkovsky effect. According to the theory of the effect the asteroid mass is to be around 8×10^{10} kg, mean density - 1.26 g/cc, porosity - 40%. Bennu itself has to have rubble pile interior [3].

The overall asteroid shape was determined from radar observations [5] after modeling simulations (fig.29). The authors came to conclusion that Bennu is a spheroid with prominent and well defined equatorial ridge. The object looks a bit faceted. Besides, the views' perimeters, especially the southern polar one, are geometrically close to a distorted quadrangle.

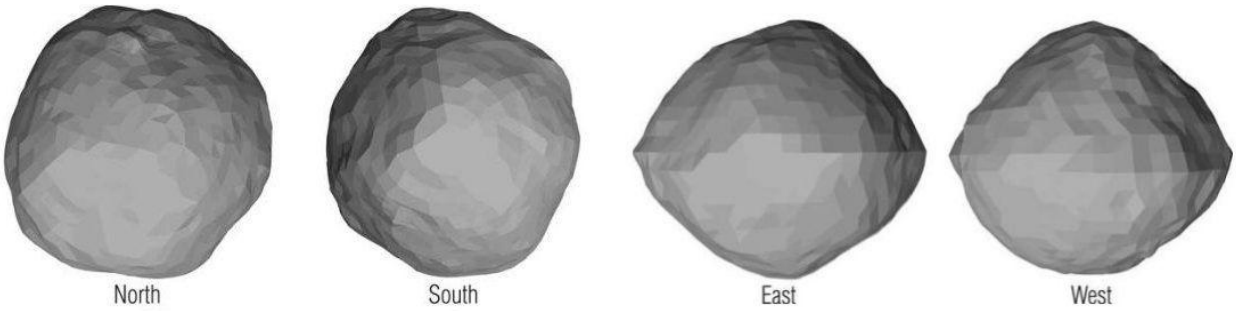

Fig.29. Radar modeled views of Bennu from the North, South, East, and West (along the main axes of inertia). The uncertainty is the largest along longitudes in polar z-axis dimension.
(fig.29 is composed of parts of fig.6 in [1]).

Lightcurve optical data [5] acquired at high phase angles (60-70°) were surprising (fig.30). They do not support pyramid-like four-fold symmetry of Bennu. Opposite, low amplitude and trimodal (three maxima and three minima) light-curves are suggestive of tetrahedron shapes.

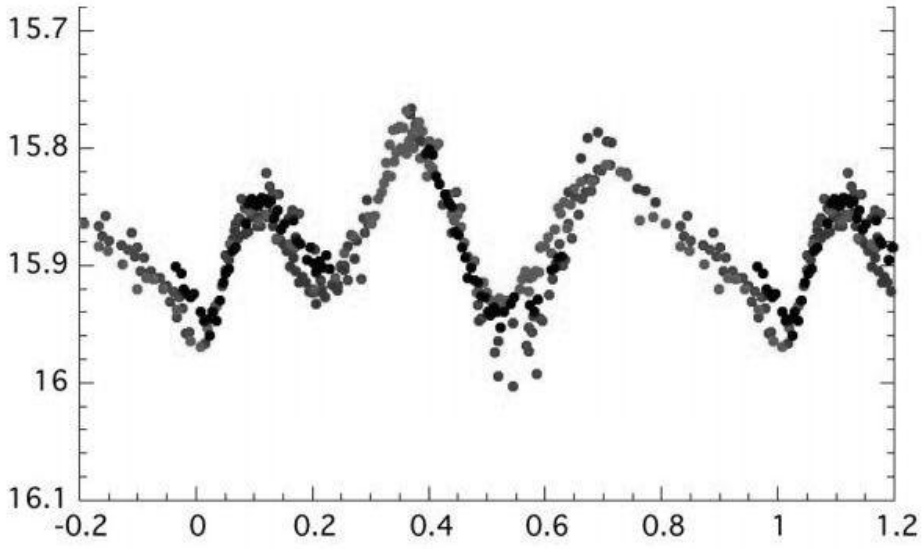

Fig.30. Composite rotational lightcurve of Bennu. Data points are results of four consecutive nights of observations in September 2005. One rotational cycle (0-1) continues 4.288 hours.
(fig.30 is the modified fig.1 from [4])

Authors of [35] found no surface albedo variations in Spitzer photometric data for wavelengths 16 and 22 micrometers. This spectral uniformity implies lack of large scale differences in surface composition of Bennu and proves that the reason of curve asymmetry is faceted irregular shape. Notice the unequal angular widths of three phase curve maxima during period of rotation, the two ones being approx. equal to the third one (fig.30).

5.2 Bennu's appearance analysis

To illustrate Bennu's lightcurve situation we photographed a stone with similar qualities. The image is given in fig. 31 (cf. polar radar views in fig.29).

Fig.31. Our image of a faceted stone with approx. four side base. The stone lightcurves would have three maxima in case of rotation around axis perpendicular to the image plane. To discern details inversion of image colors is suggested.

Relief details of Bennu determined by Arecibo and Goldstone radars are also very interesting (fig.32.). It is said in [5]: "We chose parameters that enforce a uniform mass distribution and principal-axis rotation. After some experimentation, we chose a set of smoothing parameters that allowed the shape to evolve but did not result in spiky artifacts related to features not evident in the data."

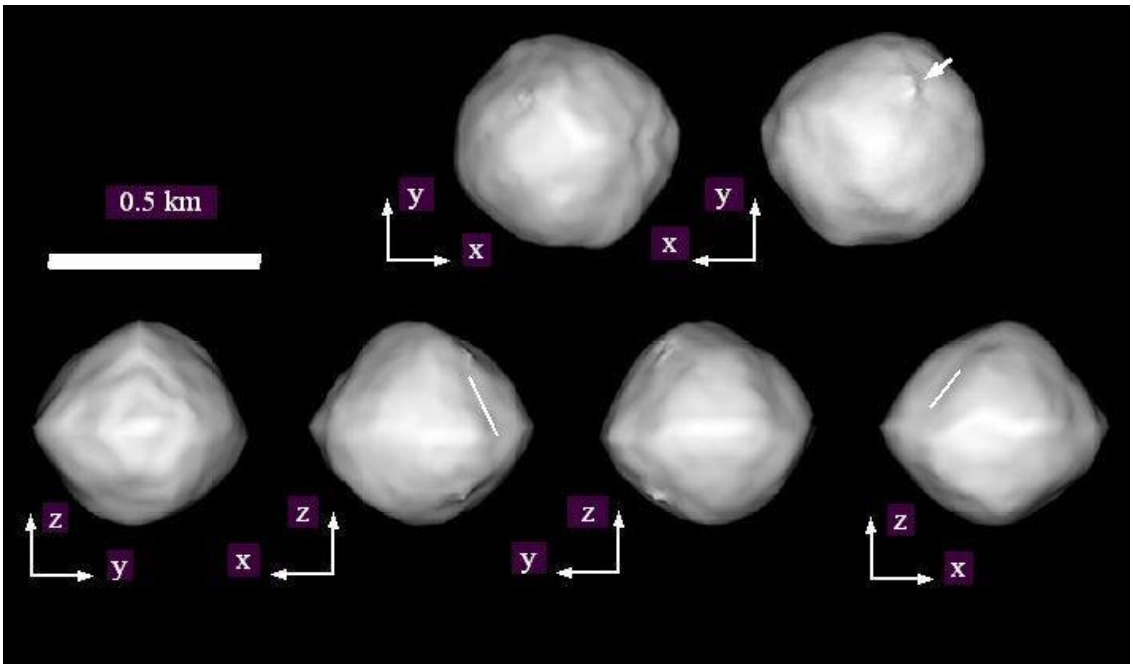

Fig.32. Six views of asteroid Bennu as it looks along principal axes of inertia. Upper row from left to right shows northern and southern polar views. Some of the apparent north-south symmetry is a model artifact that stems from the near-equatorial geometry. In the lower row the North is up. Lines mark global fault. Short arrow points to southern boulder.
(fig.32 uses parts of fig.3 from [4]).

It was pointed out earlier that radar asteroid models are reliable in the sense of existence of definite surface features, but their mutual weights depend upon simulation assumptions because a number of smoothing parameters and physical constraints are usually imposed on models. Besides, in radar images small scale features like fresh crater materials may be missed with relief topography. Thus the estimation of partly uncertain details in fig.31 is to be undertaken with care and only large features taken in account as real.

We think the asteroid originated in a result of explosive ejection the way similar to the others discussed above. Authors of Bennu's models underline its spheroid shape which proves rubble pile structure of small asteroids. But Bennu is slow rotator, compared to most primaries of the near-Earth binaries (3 hours and less). Hence theoretically Bennu has to change its rotation period because of YORP effect.

Fig.32. proves that Bennu has shapes alike other above discussed celestial bodies, especially 1999 KW4 (see fig.7). We prefer to envision more faceted diamond-like shape with larger bulge. Truncation is also not excluded. The radar model is possible to deviate from the reality either because of unique assumptions, or due to special parameters of surface reflections. For example, the blur of faceting may result from high Bennu's surface metal contents.

The global features of Bennu look familiar. For instance, angular equatorial ridge is the necessary element of ejected cone or pyramid appearance. Plastically modified at the starting moment it is to be stronger than other parts of ejected body. Equator region separates the northern cone subjected to explosive high temperature shocks while formation and initially unchanged southern region. Northern polar view should contain curved or spiral relief features, the curvature being determined by rotation direction at the start. That means dichotomy in surface composition of an ejected body. The location of the largest boulder proves that fault evolving continued in South latitudes after Bennu's formation. The origination with the South up means the southern hemisphere is older than the northern one.

Bennu as other above studied asteroids is to consist of large parts with different inner stresses that mean different evolution rate. That is why crater/boulder statistics should be varied for different lobes and facets. Global fault remnant (fig.32, lines) divides the asteroid almost by half. The largest hundred meters in dimension angular crater (face-on in down left view of fig.32.) is, as usual, located in singular region close to Bennu's main fault. Somewhat smaller bulge craters were not revealed, but they are to exist. There should be some regular ridge features genetically related to dyke or streak remnants on the ridge.

The conclusion of radar observations is that for smaller scales the shape is rather smooth with some large scale features and one prominent 10 to 20m boulder near the southern pole. According to our rationale after origination in course of Bennu's evolution the boulder was explosively thrown out with the formation of coincident crater. There should be nearby remains of similar sized crater, may be partly destructed or healed.

Except for the boulder no other small scale features were found down to 7.5m resolution of radar, but there are some hints on surface relief details at the noise level. An indirect test on fine features suggests their reality [5]. We think those relief features are to be found and to be of angular geometry as is the case for Ryugu. The reason is that they formed in stress fields connected to overall faceted shape of Bennu.

5.3 Some constraints and features

On smaller than global scales we as usual anticipate find concomitant ejected rock/crater pairs, at least their remnants. The hope is to come across freshly ejected rock bodies. Slow rotation of Bennu hints on relatively slow intensity of its geologic processes incl. ejective orogenesis. It is possible as is sometimes the case for Ryugu that ejective jumps of rocks are not necessary result in their flips. The situation is the crossing step between rock landslides and rock overturns. Slides on asteroids, planets, and even Earth are happened to be very energetic and long-distance. No surprise they are likely to be sometimes explosive.

The OSIRIS-REx mission purposes arise from widely acknowledged theories that asteroids are primitive bodies that have not changed since the times of Solar System formation. Hence asteroids are to contain its small constituents, planetesimals. Besides, the mission hopes to find pristine materials that are necessary for life i.e. carbon, water, and different organics. We think that those have been forming in the course of Bennu's evolution.

As it is usual for the largest asteroid Ceres organic materials in highest concentrations are to be found in restricted areas, near and inside craters in definite size range [33]. Some of organic materials together with other substances are to mark global lineaments of the asteroid. For Ceres this is directly proved by the planetary maps of with stripy distributions of phyllosilicate and ammonia abundances [34]. The same phenomenon universal for rock bodies of Solar system is anticipated on Bennu.

On Earth geologic discontinuities concentrate stress and as a rule alleviate fluid movement from deep insides. Fractures, cracks, and faults are prone to be filled with different impurities, inclusive substances, and even magma. We saw the reflections of those processes on Ryugu's topology, spectral, and temperature maps (figs. 15, 19, 20). Spectral data are of great value in finding direct coincidence between relief features and materials.

As for ages, the brighter boulders and their craters are younger and appear to provide bluish colors to Bennu's spectra. The southern boulder whiter colors mean its comparatively younger age as is the case for other asteroids. Our study of different asteroids shows that the brighter are the materials, the younger they are.

More to the point, we are looking forward to findings of described substance distributions exposed by x-ray maps. Regolith X-Ray Imaging Spectrometer (REXIS) will map the distribution of elements across the asteroid surface e.g. O, Fe, Mg in the range 0.5-7.5kev. Distinction of separate elements is of great importance for deciphering their diffusions and reactions in the asteroid crust.

Some sources of X-rays are anticipated to be fixed on the surface of Bennu. We also think that transients independent of solar wind are to be grasped by REXIS and other devices. Especially interesting is the impact experiment. Different optical, electromagnetic, high-energy effects are possible on different scales during it. Transients of different kinds may exist independently of the probe influence because small asteroids are more geologically active than big ones due to their quicker evolutions.

6 Discussions

6.1 Scale independence and asteroid Lutetia.

Recent observations of 0.9km wide Ryugu allow for comparison of its features with those of other asteroids. The geometry of its ridge crater resembles surface features of (21) Lutetia 100km in diameter (figs.33, 34).

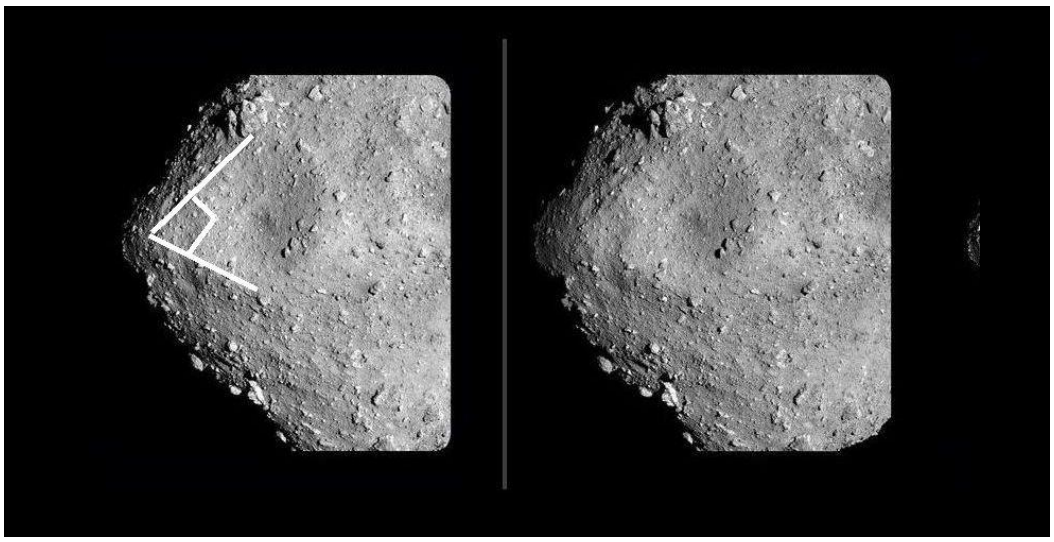

Fig.33. Binocular stereo image of the largest bulge crater on the equator of Ryugu. White lines mark relief manifestations of the crustal structure.
Image credit: Brian May.
(http://www.hayabusa2.jaxa.jp/en/topics/20180731e/index.html)

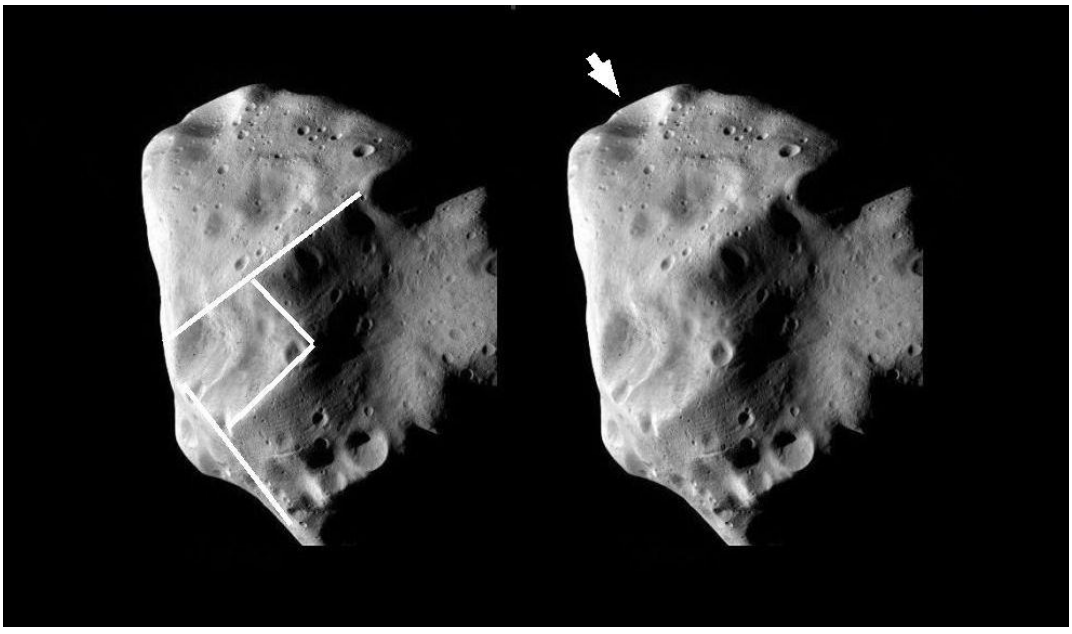

Fig.34. Two close-up images of Lutetia's northern hemisphere with complex "cratered" surface taken by ESA Rosetta spacecraft passed by on 10 July 2010. White lines mark features similar to those of Ryugu, arrow marks ridge crater.
Credit: ESA 2010 MPS for OSIRIS Team MPS/UPD/LAM/IAA/RSSD/INTA/UPM/DASP/IDA (CC BY-SA 4.0)
(https://www.flickr.com/photos/europeanspaceagency/4781143008/)

Main belt asteroid Lutetia is one of the largest asteroids ever imaged by spacecraft [36,37]. It is commonly thought of as the primitive survivor of violent birth of the Solar System. Lutetia was found to be the battered world of many craters (fig.34). Whether to think about this relief features as statistical groups of separate craters or unique relief areas is a matter of approach. Our rationale underlines the role of inner stress concentrating crustal structures in relief exposure. It is the symmetry of cracks, faults, crustal layers, and inclusions which determines the symmetry of separate craters and their fields. Thus Lutetia is to be much younger than the Solar System because it is the product of sequential evolution of larger rigid celestial bodies.

Another view of Lutetia is shown in fig.35. We changed the colors of the image for our reader to be able to discriminate relief details. The asteroid bears the features which are analogous to spinning tops, e.g. Steins or Ryugu. The line remnants of the global asteroid fault (black lines) appear to visually separate large front part of Lutetia (in fig.35) from the hidden rear bulk. Craters (arrows) mark Lutetia's equatorial bulge. A rhomb depression near it is similar to the equatorial craters of Steins. Ryugu, and others. Rhomb and triangle features are the analogs of those of Steins (cf. figs.6-8 [6]). Punctuated craters seem to continue the groove and mark global fault line.

Planar shape of Lutetia results from the parallel borders of crustal layer it casted out from. There are lots of topological analogs of the considered features on the surfaces of asteroids, comets, and satellites of different sizes. For instance, Uran's satellite Miranda comprises famous coronae (oval depressions) with open crustal layers.

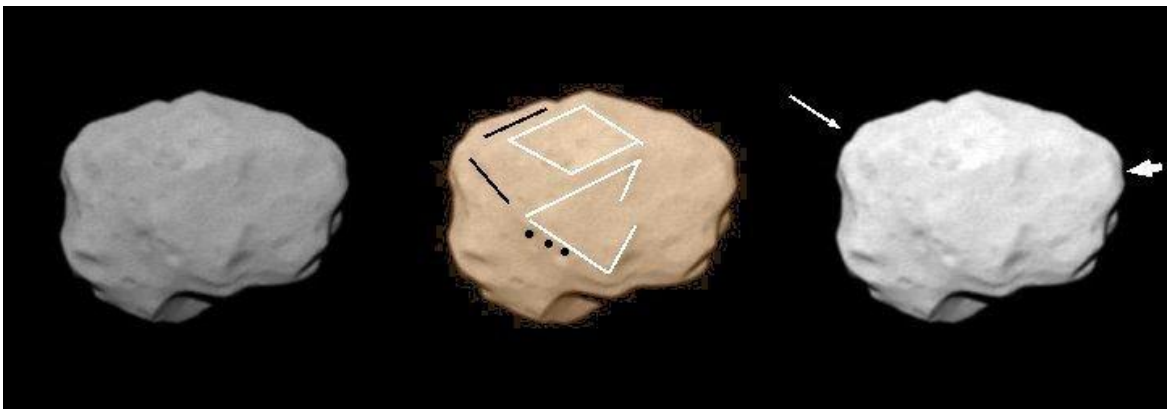

Fig.35 View of Lutetia taken by Rosetta spacecraft at a distance 36000km on 10 July 2010. Left image is the original black and white view, middle - sepia colored, right - contrasted left. Black lines show global fault groove, black points mark plausible catena as its continuation. White rhomb and white cut triangle mask tension/shear relief features. Arrows point to ridge craters (see text).
Credit: ESA 2010 MPS for OSIRIS Team MPS/UPD/LAM/IAA/RSSD/INTA/UPM/DASP/IDA (CC BY-SA4.0)
(https://www.flickr.com/photos/europeanspaceagency/4780536277/in/photostream/)

All the said is another confirmation that solid celestial bodies' evolutions include the disintegrating stages of sequential ejective orogeneses on different space scales. As wrinkles and scars on human faces surface asteroid features are the reflections of their personal histories. It is a pity we are not able to fully decipher those provenances yet.

6.2 Probable parents of near-Earth asteroids

It is commonly thought that Bennu was brought about in the inner asteroid main belt as a fragment from larger body. Ryugu and Bennu are believed to have originated in the Polana-Eulalia family complex [38]. Then orbits of both asteroids drifted as a result of Yarkovsky effect and mean motion resonances with giant planets, such as Jupiter and Saturn. Interactions with the planets as well as Yarkovsky and YORP effects modified spin, shape, and surface features of the asteroids.

We think that asteroids and all celestial solid objects are rock bodies and impossible to be rubble piles as it sometimes results from the above theories. Another contradiction is that asteroids analyzed by us are geologically fresh and young. Our alternative hypothesis states that near-Earth asteroids formed in Earth's system. This simple guess does not need complex intermediate drift and modifications of different asteroids. Possible evidences are as follows.

All near-Earth asteroids considered in this report are in quasi-resonances with Earth or close to them. That means the ratios of their orbital periods to that of Earth are given by natural digits. Revolution period of Bennu is 436.6d, Ryugu – 474d, 2008 EV5 – 343d, 1999 KW4 – 188d, Didymos – 799d, and 1994 CC – 788d. The ratios of these periods to Earth's orbital one are 1.25 (5/4), 1.3 (~4/3), 0.94 (~1/1), 0.51 (~1/2), 2.1 (~2/1), 2.1 (~2/1). Bennu's close approach to Earth repeats every 6 years, Ryugu's – 13 years, 1999 KW4 – half of year, and so on. The resonances mean energy transfer from a parent body to offspring asteroids.

Hayabusa2 team performed gravity measurements of Ryugu and announced outcome data. The mass is 4.5×10^{11}kg, the gravity is ca. 1/80,000 of Earth's one (pg.23 [30]). Due to centrifugal forces the surface acceleration ranges from 0.11 to 0.15mm/s^2 in equatorial and polar areas, respectively (pg.17 in [31]). We calculated the asteroid volume as the sum of two cones with the heights 0.44km and base radii 0.5km (pg.23 [30]). The volume is about 0.24km^3. The data allows for estimation of Ryugu's density as about 2 g/cc.

The density evaluations for Ryugu do not contradict to data on other asteroids analyzed in this article. Estimations of their densities with accuracies of several tens of percents are 3g/cc for 2008 EV5, 2g/cc - 1999 KW4, 2.1g/cc - Didymos, and 2.1g/cc - 1994 CC (see Section 3.2). We see no reasons for Bennu's density to be twice less than those. Except for observed fourteen years' change trends of its orbital semi-major axis virtually prolonged for million year periods in order to explain them by Yarkovsky effect.

Earth rock densities are 3-3.3g/cc, with 5.5g/cc being average for the planet. Average lunar density is 3.34g/cc, with crustal density 2 g/cc at depths deeper than 2m [39]. We conclude that densities of near-Earth asteroids belong to density ranges of Earth's and lunar crusts.

We speculate that near-Earth asteroids appear to appear as a result of explosive ejective fission of Earth's or the Moon's crusts. According to [40] spectra of of Ryugu [C-type] and Bennu [B-type] are similar to CM chondrite. Therefore, they are relatives and their samples will likely contain similar silicates formed under similar conditions. Petrographic and chemical similarities of the asteroids are confirmations of their formation in Earth's system. In the nearest future the hypothesis is possible to be proved or rejected by laboratory studies of isotope clocks of asteroid samples that are going to be taken by OSIRIS-REx and Hayabusa2 sample return missions.

7 Conclusions and broad contexts

In conclusion, above considerations give evidences that asteroids of different sizes and compositions formed on various space scales in evolutionary processes of the same nature. That is slow plastic deformations with simultaneous sequential explosive ejections. Our approach means the interplay of elasticity and plasticity which result in ejection/expansion development. According to this simple astrophysical model there is no need to imagine diverse evolvement stages for large celestial objects as well as no need in YORP effect for the formation of small asteroids.

The concept, that every celestial object is open system able to change energies with its ambient, lies in the heart of our rationale. In this paper we apply the ideas of synergetics, solid state physics, fracture mechanics, and nonlinear structure formations to describe objects many orders of magnitude larger than those the ideas were developed for. We see space objects as hierarchical systems with diverse feedback loops which strive to save their integrities. Superposition principle is applicable to them only in cases of small deviations from equilibrium and relatively short evolution times which scale up with their sizes.

As the next step and next approximation after conservative celestial system models this rationale is consistent with those models and sometimes gives tiny amendments to known interpretations. But in general our results contradict to widely accepted conclusions. Some of our predictions for Bennu, explanations of Ryugu and other asteroids are at drastic odds with basic knowledge about them.

Everything old is new again and our approach looks unusual only to a mainstream researcher. Hundred years ago the common notion was the hypothesis of satellite and comet formations inside their parent planets and throwing them out by planet volcanoes. The idea resulted from careful study of Earth's geology and dynamics of celestial bodies about two hundred years ago, in times of its author J.L. Lagrange and P.S. Laplace cosmogony inquiries (see also [6]). The hypothesis fully disappeared from intuition of majority of astrophysicists only in the second part of the twentieth century. After the world wars and drastic mass media development humankind was impressed by pictures of different scale explosions due to outer impacts. That explanation of crater and asteroid formation mechanisms is still dominating.

Inspired by observational data [7] our unified ejective approach is compatible with the old ideas. To date it is far from being finally developed but it does work. Whether the model is able to anticipate a bulk of observations is going to be known in the nearest future. In this sense the surplus of Hayabusa2 and OSIRIS-REx missions is that researches and curious people are getting data on Ryugu and Bennu with high rates natural to other natural sciences, if not quicker.

8 Summary of predictions

To sum up we outnumber tens of anticipated properties of asteroid Bennu. The following restrictions and constraints are by no means exhaustive. They were chosen in a bit subjective manner and are self-consistent in the frames of our integral approach:

- diamond-like shape with the northern apex angle close to 90°

- rotational axis as the axis of Bennu's symmetry

- somewhat shorter z dimensions along rotational axis compared to x or y ones

- inequality of x and y dimensions (Bennu's widths)

- plastic expansion evolution trends revealed in shape deviations

- surface material and relief North-South dichotomy

- several constituent parts of the asteroid

- curved northern relief features

- global main fault and its relief revelations which cut Bennu approx. by half

- strong equatorial mountain ridge

- angular perimeters of craters

- one largest equatorial depression close to the global fault

- approximately regular crater locations on equatorial bulge

- side differences in crater statistics

- ten meter crater concomitant to similar size boulder in southern latitudes

- obvious geometric similarities between some craters and boulders

- existence of catenae and lined chains of boulders

- relief features lined in North-South, East-West directions and 45° to them

- lined substance and temperature distributions on different scales

- recent geologic activity and fresh remnants of it

- patches of locally formed organic materials in and outside of craters

- regular distributions of boulders on different scales

- angular cliff-like shapes of boulders
- young geologic age
- solid object, not a rubble pile
- bulk rock compositions with inclusions of heavier and lighter substances
- density in the range 2-3 g/cc
- x-ray and electromagnetic transients independent of solar wind
- transients' location along lineaments and circles on different scales

References

1. Lauretta, D.S. et al.
   OSIRIS-REx: Sample Return from Asteroid (101955) Bennu
   Space Sci. Rev. Published online 28 August 2017
   doi:10.1007/s11214-017-0405-1
   Arxiv: 1702.06981

2. Lauretta, D.S. et al.
   The OSIRIS-REx target asteroid (101955) Bennu: Constraints on its physical, geological, and dynamical nature from astronomical observations
   Meteoritics & Planetary Science 50, 834–849, 2015
   doi:10.1111/maps.12353

3. Chesley, S. R. et al.
   Orbit and bulk density of the OSIRIS-REx target Asteroid (101955) Bennu
   Icarus 235, 5–22, 2014
   doi:10.1016/j.icarus.2014.02.020
   Arxiv: 1402.5573

4. Hergenrother, C.W. et al.
   The Design Reference Asteroid for the OSIRIS-REx Mission Target (101955) Bennu (An OSIRIS-REx DOCUMENT 2014-April-14)
   Arxiv: 1409.4704

5. Nolan, M.C. et al.
   Shape model and surface properties of the OSIRIS-REx target Asteroid (101955) Bennu from radar and lightcurve observations
   Icarus 226, 629–640, 2013
   doi:10.1016/j.icarus.2013.05.028

6. Soumbatov-Gur, A.
   Diamonds in the sky. Why ?
   Research Report 2018. HAL-01751079v2
   https://hal.archives-ouvertes.fr/hal-01751079v2/document

7. Soumbatov Gur, A.
   Moving mountains and white spots of Ceres.
   Arxiv: 1712.01320

8. Garvin, J. et.al.
   Linne: simple lunar mare crater from LRO observations
   42nd Lunar and Planetary Science Conference, 2063.pdf, 2011

9 Asphaug, E. et al.
   Asteroid Interiors
   Chapter in book “Asteroids III”, eds. Bottke, W. F. Jr. et al.
   (Tucson: Univ. Arizona Press), 463-484, 2002

10. Pisani, E. et al.
Puzzling Asteroid Families
Icarus 142, 78–88, 1999
Article ID icar.1999.6205, available online at http://www.idealibrary.com

11. Jacobson, S.A. et.al.
Effect of rotational disruption on the size-frequency distribution of the Main Belt asteroid population
MNRASL 439, L95-L99, 2014
doi:10.1093/mnrasl/slu006

12. Dermott, S.F. et al.
The common origin of family and non-family asteroids
Nature Astronomy 2, 549-554, 2018
doi:10.1038/s41550-018-0482-4

13. Accomazzo, A. et al.
The flyby of Rosetta at asteroid Steins – mission and science operations.
Planetary and Space Science 58, 1058–1065, 2010
doi:10.1016/j.pss.2010.02.004

14. Jorda, L. et al.
Steins: Shape, topography and global physical properties from OSIRIS observations.
Icarus 221, 1089–1100, 2012
doi:10.1016/j.icarus.2012.07.035

15. Busch, M. W. et al.
Radar observations and the shape of near-Earth asteroid 2008 EV5
Icarus 212, 649–660, 2011
doi:10.1016/j.icarus.2011.01.013
Arxiv: 1101.3794

16. Ostro, S. J. et al.
Radar Imaging of Binary Near-Earth Asteroid (66391) 1999 KW4
Science 314, 1276-1280, 2006
doi:10.1126/science.1133622

17. Scheeres, D. J. et al.
Dynamical Configuration of Binary Near-Earth Asteroid (66391) 1999 KW4
Science 314, 1280-1283, 2006
doi:10.1126/science.1133599

18. Campo Bagatin, A. et al.
Dynamical and Physical Properties of 65803 Didymos, the AIDA Mission Target
European Planetary Science Congress 11, 846, 2017

19. Brozovic, M. et al.
Radar and optical observations and physical modeling of triple near-Earth Asteroid (136617) 1994 CC
Icarus 216, 241–256, 2011
doi:10.1016/j.icarus.2011.09.002

20. Wada, K. et al.
Asteroid Ryugu before the Hayabusa2 encounter
ArXiv: 1804.03734

21. Tsuda, Y. et al.
Hayabusa2–Sample return and kinetic impact mission to near-Earth asteroid Ryugu
Acta Astronautica, 2018
doi.org/10.1016/j.actaastro.2018.01.030

22. Campins, H. et al.
Spitzer observations of spacecraft target 162173 (1999 JU3)
Astronomy & Astrophysics 503, L17–L20, 2009
doi:10.1051/0004-6361/200912374
Arxiv: 0908.0796

23. Lange, C. et al
Exploring small bodies: Nano- and microlander options derived from the Mobile Asteroid Surface Scout
Advances in Space Research, 2018
doi:10.1016/j.asr.2018.05.013
Available online at www.sciencedirect.com

24. Grott, M. et al.
The MASCOT radiometer MARA for the Hayabusa 2 mission.
Space Sci. Rev. 208, 413-431, 2017
doi:10.1007/s11214-016-0272-1

25. Herčík, D. et al.
The MASCOT magnetometer.
Space Sci. Rev. 208, 433-449, 2017
doi:10.1007/s11214-016-0236-5

26. Müller, T. G. et al.
Hayabusa-2 mission target asteroid 162173 Ryugu (1999 JU3): Searching for the object's spin-axis orientation.
Astronomy and Astrophysics, 599, A103, 1-25, 2017
doi:10.1051/0004-6361/201629134
ArXiv: 1611.05625

27. Vilas, F.
Spectral characteristics of Hayabusa2 near-Earth asteroid targets 162173 1999 JU3 and 2001 QC34.
The Astronomical Journal, 135,1101–1105, 2008
doi:10.1088/0004-6256/135/4/1101

28. Operation status for the asteroid explorer, Hayabusa2, in the vicinity of Ryugu
JAXA Hayabusa2 Project, Press release, July 19, 2018!
http://www.hayabusa2.jaxa.jp/en/enjoy/material/press/Hayabusa2_Press20180719_ver7_en.pdf

29. Operation status for the asteroid explorer, Hayabusa2, in the vicinity of Ryugu
JAXA Hayabusa2 Project, Press release, August 2, 2018
http://www.hayabusa2.jaxa.jp/en/enjoy/material/press/Hayabusa2_Press20180802_ver6_en3.pdf

30. Candidates for landing sites for the Hayabusa2 mission
JAXA Hayabusa2 Project, Press release, August 23, 2018
http://www.hayabusa2.jaxa.jp/en/enjoy/material/press/Hayabusa2_Press20180823_ver6_e.pdf

31. Operation status for the asteroid explorer, Hayabusa2, in the vicinity of Ryugu
JAXA Hayabusa2 Project, Press release, September 5, 2018
http://www.hayabusa2.jaxa.jp/en/enjoy/material/press/Hayabusa2_Press20180905_E_verL2.pdf

32. Wallis, M.K, Wickramasinghe, N.C.
Rosetta Images of Comet 67P/Churyumov–Gerasimenko: Inferences from Its Terrain and Structure.
Astrobiology & Outreach 3(1), 1000127, 2015.
doi:10.4172/2332-2519.1000127
http://dx.doi.org/10.4172/2332-2519.1000127

33. Kaplan, H.H., et al.
New constraints on the abundance and composition of organic matter on Ceres.
Geophysical Research Letters, 45(11), 5274-6782, 2018
doi:10.1029/2018GL077913

34. Ammanito, E. et.al.
Distribution of phyllosilicates on the surface of Ceres.
Science 353 (6303), aaf 4279, 2016.
doi:10.1126/science.aaf4279

35. Emery, J.P. et al
Thermophysical characterization of potential spacecraft target (101955) 1999 RQ36.
41st Lunar and Planetary Science Conference, 2282.pdf, 2010

36. Sierks, H. et al.
Images of Asteroid 21 Lutetia: A Remnant Planetesimal from the Early Solar System
Science 334, 487-490, 2011
doi:10.1126/science.1207325

37. Pätzold, M. et al.
Asteroid 21 Lutetia: Low Mass, High Density
Science 334, 491–492, 2011
doi:10.1126/science.1209389

38. de León, J. et al.
Expected spectral characteristics of (101955) Bennu and (162173) Ryugu, targets of the OSIRIS-REx and Hayabusa2 missions
Icarus 313, 25-37, 2018
doi:10.1016/j.icarus.2018.05.009
Arxiv: 1805.08774

39. Slyuta E. N.
Physical and Mechanical Properties of the Lunar Soil (A Review)
Solar System Research 48(5), 330–353, 2014
doi:10.1134/S0038094614050050

40. Schrader, D.L., Davidson, J.
CM and CO chondrites: A common parent body or asteroidal neighbors? Insights from chondrule silicates
Geochimica et Cosmochimica Acta, 214, 157-171, 2017
doi:10.1016/j.gca.2017.07.031